Journal of Alzheimer's Disease xx (2021) x–xx
DOI 10.3233/JAD-201271
IOS Press

Resting State Alpha Electroencephalographic Rhythms Are Differently Related to Aging in Cognitively Unimpaired Seniors and Patients with Alzheimer's Disease and Amnesic Mild Cognitive Impairment

Claudio Babiloni[a,b,*], Raffaele Ferri[c], Giuseppe Noce[d], Roberta Lizio[d], Susanna Lopez[a], Ivan Lorenzo[c], Federico Tucci[a], Andrea Soricelli[d,e], Flavio Nobili[f,g], Dario Arnaldi[f,g], Francesco Famà[f], Francesco Orzi[h], Carla Buttinelli[h], Franco Giubilei[h], Virginia Cipollini[h], Moira Marizzoni[i], Bahar Güntekin[j,k], Tuba Aktürk[k], Lutfu Hanoğlu[l], Görsev Yener[m,n], Yağmur Özbek[n], Fabrizio Stocchi[o], Laura Vacca[o], Giovanni B. Frisoni[i,p] and Claudio Del Percio[a]

[a]*Department of Physiology and Pharmacology "Vittorio Erspamer", Sapienza University of Rome, Rome, Italy*
[b]*San Raffaele of Cassino, Cassino (FR), Italy*
[c]*Oasi Research Institute - IRCCS, Troina, Italy*
[d]*IRCCS SDN, Napoli, Italy*
[e]*Department of Motor Sciences and Healthiness, University of Naples Parthenope, Naples, Italy*
[f]*Clinica Neurologica, IRCCS Ospedale Policlinico San Martino, Genova, Italy*
[g]*Dipartimento di Neuroscienze, Oftalmologia, Genetica, Riabilitazione e Scienze Materno-infantili (DiNOGMI), Università di Genova, Italy*
[h]*Department of Neuroscience, Mental Health and Sensory Organs, Sapienza University of Rome, Rome, Italy*
[i]*Laboratory of Alzheimer's Neuroimaging and Epidemiology, IRCCS Istituto Centro San Giovanni di Dio Fatebenefratelli, Brescia, Italy*
[j]*Department of Biophysics, School of Medicine, Istanbul Medipol University, Istanbul, Turkey*
[k]*REMER, Clinical Electrophysiology, Neuroimaging and Neuromodulation Laboratory, Istanbul Medipol University, Istanbul, Turkey*
[l]*Department of Neurology, School of Medicine, Istanbul Medipol University, Istanbul, Turkey*
[m]*Izmir Biomedicine and Genome Center, Dokuz Eylul University Health Campus, Izmir, Turkey*
[n]*Department of Neurosciences, Institute of Health Sciences, Dokuz Eylul University, Izmir, Turkey*
[o]*Institute for Research and Medical Care, IRCCS San Raffaele Pisana, Rome, Italy*
[p]*Memory Clinic and LANVIE - Laboratory of Neuroimaging of Aging, University Hospitals and University of Geneva, Geneva, Switzerland*

Accepted 14 May 2021

*Correspondence to: Prof. Claudio Babiloni, PhD, Department of Physiology and Pharmacology "V. Erspamer", Sapienza University of Rome, P. le A. Moro 5, 00185, Rome, Italy. Tel.: +39 0649910989; E-mail: claudio.babiloni@uniroma1.it.

ISSN 1387-2877/$35.00

Abstract.

Background: In relaxed adults, staying in quiet wakefulness at eyes closed is related to the so-called resting state electroencephalographic (rsEEG) rhythms, showing the highest amplitude in posterior areas at alpha frequencies (8–13 Hz).

Objective: Here we tested the hypothesis that age may affect rsEEG alpha (8–12 Hz) rhythms recorded in normal elderly (Nold) seniors and patients with mild cognitive impairment due to Alzheimer's disease (ADMCI).

Methods: Clinical and rsEEG datasets in 63 ADMCI and 60 Nold individuals (matched for demography, education, and gender) were taken from an international archive. The rsEEG rhythms were investigated at individual delta, theta, and alpha frequency bands, as well as fixed beta (14–30 Hz) and gamma (30–40 Hz) bands. Each group was stratified into three subgroups based on age ranges (i.e., tertiles).

Results: As compared to the younger Nold subgroups, the older one showed greater reductions in the rsEEG alpha rhythms with major topographical effects in posterior regions. On the contrary, in relation to the younger ADMCI subgroups, the older one displayed a lesser reduction in those rhythms. Notably, the ADMCI subgroups pointed to similar cerebrospinal fluid AD diagnostic biomarkers, gray and white matter brain lesions revealed by neuroimaging, and clinical and neuropsychological scores.

Conclusion: The present results suggest that age may represent a deranging factor for dominant rsEEG alpha rhythms in Nold seniors, while rsEEG alpha rhythms in ADMCI patients may be more affected by the disease variants related to earlier versus later onset of the AD.

Keywords: Aging, exact Low-resolution brain electromagnetic source tomography, mild cognitive impairment due to Alzheimer's disease, resting state electroencephalographic rhythms

INTRODUCTION

In relaxed adults, staying in quiet wakefulness at eyes closed in a silent room is related to the so-called resting state electroencephalographic (rsEEG) rhythms [1]. The highest amplitude of these rhythms is observed in posterior areas at alpha frequencies (8–13 Hz) [1].

The rsEEG alpha rhythms reflect cortical neural synchronization mechanisms underpinning the inhibition of sensory, cognitive, and motor areas in the parietal, temporal, and occipital cortex during a condition of low vigilance [2, 3]. The higher the amplitude of alpha rhythms, the greater the cortical synchronization at alpha frequencies, and the higher the local cortical inhibition [1]. Sub-bands of these rhythms may have different functions. Alpha rhythms at low frequencies (8–10.5 Hz) may mainly reflect cortical neural synchronization mechanisms moderating brain arousal, expectancy, and readiness [4], whereas alpha rhythms at high frequencies (10.5–13 Hz) may mainly reflect those mechanisms moderating episodic memory processes [4].

As compared to rsEEG alpha rhythms, those oscillating at delta (1–4 Hz) and theta (4–7 Hz) frequencies show smaller amplitude. During event-related cognitive information processing, alpha rhythms disappear, while delta and theta increase amplitude, especially in frontal areas [5]. In parallel, faster beta (13–30 Hz) and gamma (30–70 Hz) rhythms increase in amplitude over task-related cortical regions. These high-frequency rhythms may be enhanced by forebrain cholinergic inputs to the hippocampal, thalamocortical, and cortical neurons [6].

The mentioned rsEEG rhythms manifest changes in magnitude and frequencies along physiological aging and Alzheimer's disease (AD) progression [1, 7–9]. Physiological aging is characterized by the following modifications in cognitively unimpaired healthy elderly (Nold) seniors: 1) decreased dominant frequency of alpha rhythms from about 9 to 8 Hz [10, 11]; 2) less evident alpha waveforms [12] associated with lower spectral power density in the alpha range [4, 7, 13, 14], especially in posterior regions [15]. During physiological aging, higher-frequency alpha sources in occipito-parietal regions spatially widen, while low-frequency alpha sources in occipito-temporal regions move anteriorly [11]; 3) smaller magnitude reactivity of alpha rhythms during the eyes opening [12, 14]; and 4) intermittent rsEEG rhythms at delta or theta frequencies, abnormally reactive during eyes opening [16].

Physiological aging is also characterized by contradictory effects on other rsEEG rhythms. Delta rhythms were reported as decreased [17], increased [14], or stable [18] in amplitude. Analogously, theta and beta rhythms were reported as decreased [19] or increased [7, 18].

AD-related pathological aging was characterized by significant changes in rsEEG rhythms, especially

at delta, theta, and alpha frequencies. As compared to cognitively unimpaired elderly (Nold) seniors, patients with AD dementia (ADD) showed the following derangement in rsEEG rhythms: 1) widespread decrease in the magnitude of alpha and beta rhythms; 2) widespread increase in the magnitude of theta and delta rhythms; 3) decreased dominant alpha frequency to 8-7 Hz [20, 21]; and 4) smaller magnitude reactivity of alpha rhythms during the eye opening [21].

To investigate spatial features of the above effects, cortical sources of the rsEEG rhythms were estimated. As compared to Nold controls, ADD patients showed reduced parieto-occipital dominant alpha source activity and increased low-frequency (delta/theta) source activity in occipital, parietal, and temporal areas, as a function of *APOE4*, cognitive impairment, and structural brain impairment [22–29].

Similar changes in rsEEG rhythms were observed in patients with amnesic mild cognitive impairment (aMCI), typically having a high risk of progression to ADD [8, 27]. It was reported that occipital theta and frontal delta source activities were greater, and alpha source activities were smaller in aMCI patients than Nold seniors and elderly persons with subjective memory complaints (SMC) [30]. Furthermore, alpha source activities were smaller in aMCI patients who showed the gene coding for cystatin C (CST3 B) or *APOE4* carriers than in aMCI patients without those carriers [31, 32]. Notably, it is well known that both genotypes are associated with an increased risk of ADD.

Summarizing, the above studies showed converging and robust evidence that rsEEG alpha rhythms change their peak frequency and/or magnitude in physiological aging and AD progression. However, it is still poorly understood the interaction between age and AD. It is expected based on previous neuroimaging studies carried out in young and older Nold seniors and AD patients, as topographical (posterior versus widespread) and frequency (delta-theta versus alpha-beta) features of rsEEG rhythms were shown to be related to structural and functional magnetic resonance imaging (MRI) biomarkers of cortical neurodegenerations in patients with mild cognitive impairment due to Alzheimer's disease (ADMCI) and ADD [25, 33]. Indeed, it was shown that structural MRI evidence pointed to age effects on medial lobe atrophy steeper in ADMCI and ADD patients than Nold seniors (mean ages from 62 to 69 years) [34]. Furthermore, parietal and cingulate cortical atrophy increased with age in ADMCI and Nold seniors, while ADD patients showed the maximum atrophy in those areas regardless the age [34]. Other MRI evidence in Nold and ADD seniors ranging from 55 to 90 years (mean ages from 64 to 74 years) unveiled an addictive effect of aging and AD on the gray matter (GM) atrophy in several regions; as an exception, frontal areas showed differences in GM atrophy more specific to the effect of age [35]. In Nold seniors (mean age of 76 years), the same addictive effect was observed among cerebrospinal fluid (CSF) biomarkers of AD neuropathology, the functioning of default mode network (DMN), and white matter (WM) microstructure, the latter ones revealed by structural and functional MRIs [36]. Furthermore, positron emission tomography showed more rapid increment and accumulation of tau in frontal areas in ADD than Nold seniors ranging from 48 to 93 years (mean ages from 63 to 77 years) [37]. Moreover, it was shown that the hippocampus and the amygdala pointed to greater impairment over time in younger Nold senior with than without ε4 carriers ranging from 55 to 75 years (mean ages from 71 to 72 years) [38]. This effect was not observed in older Nold seniors and ADMCI patients ranging from 80 to 92 years (mean ages from 82 to 84 years) not progressing to dementia for 3 years [38].

The present retrospective and exploratory study investigated a possible age and AD interaction on rsEEG rhythms in Nold and ADMCI seniors. Specifically, we tested the hypothesis that as compared to the younger Nold seniors, the older ones may be associated with slowing in the alpha peak frequency and lower magnitude in rsEEG alpha rhythms as an effect of physiological aging. Furthermore, in relation to the younger ADMCI seniors, the older ones may be related to the same changes predicted in the older Nold seniors, plus effects induced by AD-related neuropathology and neurodegeneration.

The experimental design for testing the above hypothesis also considered the effect of the age factor on several relevant AD hallmarks: genetic (i.e., *APOE4*), cerebrospinal fluid (i.e., $A\beta_{42}$, t-tau, p-tau, and $A\beta_{42}$/p-tau), anthropometric (i.e., weight, height, and body mass index), cardiocirculatory (i.e., systolic pressure, diastolic pressure, pulse pressure, mean arterial pressure, and heart frequency), and neuroanatomical (i.e., volumetric and cerebrovascular). Notably, previous studies investigating the effect of age on rsEEG activity in the Nold and ADMCI groups (see the above paragraphs for the references) did not consider them altogether. Controlling those variables and separating the effects of age and AD on

rsEEG rhythms is important for the use of rsEEG biomarkers in clinical trials. These biomarkers are cost-effective and repeatable for the prediction and monitoring of clinical progression in ADMCI and ADD patients [39]. Especially for exploratory studies without the resources for serial recordings of structural and functional MRI or ^{18}F-fluorodeoxyglucose positron emission tomography (FDG-PET).

MATERIALS AND METHODS

The present study was developed based on the data of The PDWAVES Consortium (http://www.pdwaves.eu) with some datasets of the FP7-IMI "PharmaCog" (http://www.pharmacog.org) project. In the Web sites between brackets, one can find more details on the aims of the original clinical investigations at the basis of present study, the context of the original data collection, and the previous publications by the present Consortium.

Participants and diagnostic criteria

To test the study hypotheses, we used the data of an international archive, formed by clinical, neuropsychological, anthropometric, genetic, CSF, MRI, and rsEEG markers in 60 Nold seniors (mean age: 69.5 ± 0.8 SE years; age range: 52–81 years 27 male; mean education: 10.3 ± 0.5 SE years; Mini-Mental State Evaluation (MMSE) score: 28.5 ± 0.1 SE) and 63 ADMCI patients (mean age: 69.7 ± 0.8 SE years; age range: 56–81 years 30 male; mean education: 10.7 ± 0.5 SE years; MMSE score: 25.2 ± 0.3 SE). The Nold and ADMCI groups were carefully matched for age, gender, and education. Statistical analyses ($p < 0.05$) were performed to evaluate the presence or absence of statistically significant differences ($p < 0.05$) between the two groups for the age (T-test), gender (Fisher test), educational attainment (T-test), and MMSE score (Mann Whitney U test). As expected, a statistically significant difference was found for the MMSE score ($p < 0.00001$), showing a higher score in the Nold than the ADMCI group. On the contrary, no statistically significant differences were found for the age, gender, and educational attainment between the groups ($p > 0.05$).

These subjects were recruited by the following Italian and Turkish clinical units: the Sapienza University of Rome (Italy), Institute for Research and Evidence-based Care (IRCCS) "Fatebenefratelli" of Brescia (Italy), IRCCS SDN of Naples (Italy), IRCCS Oasi Maria SS of Troina (Italy), IRCCS Ospedale Policlinico San Martino and DINOGMI (University of Genova, Italy), Hospital San Raffaele of Cassino (Italy), IRCCS San Raffaele Pisana of Rome (Italy) and Medipol University of Istanbul (Turkey).

Local institutional Ethics Committees approved the present observational study. All experiments were performed with the informed and overt consent of each participant or caregiver, in line with the Code of Ethics of the World Medical Association (Declaration of Helsinki) and the standards established by the local Institutional Review Board.

The status of the ADMCI was based on the "positivity" to one or more of the following biomarkers: $A\beta_{1\text{-}42}$/phospho-tau ratio ($A\beta_{42}$/p-tau) in the CSF, FDG-PET, and structural MRI of the hippocampus, parietal, temporal, and posterior cingulate regions [40]. The "positivity" was judged by the physicians in charge for releasing the clinical diagnosis to the patients, according to the local diagnostic routine of the participating clinical Units.

The clinical inclusion criteria of the ADMCI patients were as follows: 1) age of 55–90 years; 2) reported memory complaints by the patient and/or a relative; 3) MMSE score of 24 or higher; 4) Clinical Dementia Rating score of 0.5 (CDR) [41]; 5) logical memory test [42] score of 1.5 standard deviations (SD) below the mean adjusted for age; the cognitive deficits did not have to significantly interfere with the functional independence in the activities of the daily living; 6) Geriatric Depression Scale (15-item GDS) [43] score of 5 or lower; 7) modified Hachinski ischemia [44] score of 4 or lower and education of 5 years or higher; and 8) single or multi-domain amnesic MCI status.

The clinical exclusion criteria of the ADMCI patients were as follows: 1) other significant systemic, psychiatric, and neurological illness; 2) any form of dementia or mixed dementia; 3) actual participation in a clinical trial using disease-modifying drugs; 4) systematic use of antidepressant drugs with anticholinergic side effects; 5) chronic use of neuroleptics, narcotics, analgesics, sedatives or hypnotics; 6) and anti-parkinsonian medications (cholinesterase inhibitors and memantine allowed); 7) diagnosis of epilepsy or report of seizures or epileptiform EEG signatures in the past, and 8) major depression disorders described in the Diagnostic and Statistical Manual of Mental Disorders (DSM-5).

In all ADMCI patients, AD-relevant CSF biomarkers were assessed in the framework of a neurobiological definition of AD in line with the NIA-AA Research Framework [45]. The CSF samples were

preprocessed, frozen, and stored in line with the Alzheimer's Association Quality Control Programme for CSF biomarkers [46]. Dedicated single-parameter colorimetric enzyme-linked immunosorbent assay ELISA kits (Innogenetics, Ghent, Belgium) were used to measure amyloid beta 1–42 (i.e., $A\beta_{42}$). Levels of the protein tau (i.e., total tau, t-tau) and a phosphorylated form of tau at residue 181 (i.e., p-tau) were also measured. From one frozen aliquot of CSF, the assays were run parallel according to the manufacturer's instructions. Each sample was assessed in duplicate. A sigmoidal standard curve was plotted to allow the quantitative expression (pg mL^{-1}) of measured light absorbance. All ADMCI patients of the present study were "positive" to the CSF $A\beta_{42}$/p-tau biomarker with a threshold defined in a previous investigation of our Workgroup [47]. In that investigation, the cut-off of "positivity" to that CSF $A\beta_{42}$/p-tau biomarker was 15.2 for *APOE4* carriers and 8.9 for *APOE4* non-carriers [47]. In the present study, all ADMCI patients with *APOE4* status had the CSF $A\beta_{42}$/p-tau lower than 15.2, whereas the ADMCI patients without *APOE4* status had the CSF $A\beta_{42}$/p-tau lower than 8.9.

Furthermore, in all ADMCI patients, relevant MRI markers were measured. All MRI scans were performed using 3.0 Tesla machines. The MRI protocol consisted of several acquisitions, including two anatomical T1, anatomical T2, fluid-attenuated inversion recovery (FLAIR), diffusion tensor imaging scans. Only anatomical T1 and FLAIR scans were available for all units and were analyzed in the present study.

In the centralized analysis of the MRIs, all data were visually inspected for quality assurance before the extraction of the MRI biomarkers. Specifically, we checked that there were no gross partial brain coverage errors and no major visible artefacts, including motion, wrap around, radio frequency interference, and signal intensity or contrast inhomogeneities. The two anatomical T1 scans were averaged, and the anatomical scans obtained were analyzed using FreeSurfer version 5.1.0 to automatically generate: 1) volumes of the total GM, total WM, caudate, putamen, pallidum, accumbens, hippocampus, amygdala, and lateral ventricle; 2) cortical thicknesses of the total and entorhinal cortex; and 3) WM hypointensity [48, 49]. The volumes were normalized with reference to the total intracranial volume (TIV). Furthermore, the FLAIR scan was analyzed using FMRIB Software Library (FSL) version 5.0.3 to evaluate WM lesions.

Furthermore, *APOE4* genotyping, anthropometric features (i.e., weight, height, and body mass index) and cardiocirculatory markers (i.e., systolic pressure, diastolic pressure, pulse pressure, mean arterial pressure, and heart frequency) were also measured.

In all ADMCI patients, the global cognitive status and the performance in various cognitive domains including, memory, language, executive function, planning, visuospatial function, and attention, were assessed. All ADMCI patients showed a significant reduction in the performance in at least one test of episodic memory, in most cases associated with a significant reduction in the performance at tests probing other cognitive domains. In the following, we report the neuropsychological tests administrated to the ADMCI patients in all clinical units of this study: 1) the global cognitive status was tested by the MMSE and the Alzheimer's Disease Assessment Scale–Cognitive Subscale (ADAS-Cog) [50, 51]; 2) the episodic memory was assessed by the immediate and delayed recall of Rey Auditory Verbal Learning Test [52]; 3) the executive functions and attention were evaluated by the Trail making test (TMT) parts A and B [53]; 4) the language was tested by 1-min Verbal fluency test for letters [54] and 1-min Verbal fluency test for category (fruits, animals, or car trades) [54]; and 5) planning abilities and visuospatial functions were assessed by Clock drawing and copy test [55].

All Nold seniors underwent an interview and cognitive screening (including MMSE and GDS) as well as physical and neurological examinations to exclude subjective memory complaints (SMC), cognitive deficits, and mood disorders. All Nold seniors had the MMSE score equal to or greater than 27, a CDR score equal to 0, and a GDS score lower than the threshold of 5 (no depression) or were evaluated as having no depression after an interview with a physician or clinical psychologist at the time of the enrolment. The Nold seniors with a history of previous or present neurological or psychiatric disease were also excluded. Furthermore, the Nold seniors affected by any chronic systemic illnesses (e.g., diabetes mellitus) were excluded, as were the Nold seniors taking chronically psychoactive drugs. Unfortunately, MRI, CSF, *APOE4* genotyping, anthropometric and cardiocirculatory markers were not available for Nold seniors.

Stratification of Nold seniors and ADMCI patients according to the age in tertiles

To test the effect of the aging on the rsEEG activations, the enrolled Nold seniors and ADMCI patients

Table 1
Mean values (± standard error of the mean, SE) of the demographic and clinical data as well as the results of their statistical comparisons ($p < 0.05$) in the healthy cognitively unimpaired (Nold) seniors and patients with Alzheimer's disease and mild cognitive impairment (ADMCI), stratified according to the age in youngest age tertile (Nold 1st tertile, $N = 20$; ADMCI 1st tertile, $N = 21$), median age tertile (Nold 2nd tertile, $N = 20$; ADMCI 2nd tertile, $N = 21$), and oldest age tertile (Nold 3rd tertile, $N = 20$; ADMCI 3rd tertile, $N = 21$). MMSE, Mini-Mental State Evaluation; M/F, males/females; n.s., not significant ($p > 0.05$ corrected)

Demographic and clinical data in Nold seniors and ADMCI patients				
	Nold 1st tertile	Nold 2nd tertile	Nold 3rd tertile	Statistical analysis
N	20	20	20	-
Age (y)	62.5 ± 0.8 SE	69.2 ± 0.5 SE	77.1 ± 0.5 SE	ANOVA: $F = 141.8$, $p < 0.000001$
Range of age (y)	52–66	67–73	74–81	
Gender (M/F)	8/12	9/11	10/10	Freeman Halton test: n.s.
Education (y)	10.4 ± 0.9 SE	10.2 ± 0.8 SE	10.3 ± 0.9 SE	ANOVA: n.s.
MMSE	28.8 ± 0.2 SE	28.4 ± 0.3 SE	28.4 ± 0.2 SE	Kruskal-Wallis ANOVA: n.s.
	ADMCI 1st tertile	ADMCI 2nd tertile	ADMCI 3rd tertile	
N	21	21	21	-
Age (y)	62.6 ± 0.8 SE	70.0 ± 0.3 SE	76.5 ± 0.5 SE	ANOVA: $F = 132.8$, $p < 0.000001$
Range of age (y)	56–67	68–72	73–81	
Gender (M/F)	10/11	10/11	10/11	Freeman Halton test: n.s.
Education (y)	10.8 ± 0.9 SE	10.8 ± 1.0 SE	10.6 ± 0.9 SE	ANOVA: n.s.
MMSE	25.2 ± 0.4 SE	25.4 ± 0.5 SE	25.2 ± 0.3 SE	Kruskal-Wallis ANOVA: n.s.

were stratified according to the age in the following tertiles: youngest age tertile (Nold 1st tertile, age range: 52–66 years, $N = 20$; ADMCI 1st tertile, age range: 56–67 years, $N = 21$), median age tertile (Nold 2nd tertile, age range: 67–73 years, $N = 20$; ADMCI 2nd tertile, age range: 68–72 years, $N = 21$), and oldest age tertile (Nold 3rd tertile, age range: 74–81 years, $N = 20$; ADMCI 3rd tertile, age range:73–81 years, $N = 21$). This arbitrary stratification allowed us to obtain to test the main study hypothesis with three subgroups of Nold seniors and three subgroups of ADMCI patients matched as mean age, mean education attainment, and gender. Furthermore, the three ADMCI subgroups were also matched as global cognitive status as revealed by the MMSE score. As reported in the following, we also performed a control analysis using age as a continuous variable to cross-validate the results.

Table 1 summarizes the most relevant demographic (i.e., age, gender, and education attainment) and clinical (i.e., MMSE score) features in the Nold and ADMCI tertiles. Furthermore, Table 1 reports the results of the presence or absence of statistically significant differences (exploratory $p < 0.05$ uncorrected) among the tertiles for both Nold and ADMCI groups (i.e., Nold 1st tertile versus Nold 2nd tertile versus Nold 3rd tertile; ADMCI 1st tertile versus ADMCI 2nd tertile versus ADMCI 3rd tertile) for the age (ANOVA), gender (Freeman Halton test), education attainment (ANOVA), and MMSE score (Kruskal-Wallis ANOVA). As expected, based on the stratification criterion, a statistically significant age difference was found among the tertiles for both Nold and ADMCI groups considered separately (Nold: $F = 141.8$, $p < 0.000001$; ADMCI: $F = 132.8$, $p < 0.000001$). On the contrary, no statistically significant differences were found for the education, gender, and MMSE score among the tertiles for both Nold and ADMCI groups, considered separately ($p > 0.05$). Furthermore, no statistically significant differences were found for the age, education, and gender between Nold 1st tertile versus ADMCI 1st tertile, Nold 2nd tertile versus ADMCI 2nd tertile, and Nold 3rd tertile versus ADMCI 3rd tertile ($p > 0.05$).

Moreover, in all ADMCI patients, the use of selective serotonin reuptake inhibitors (SSRIs), selective serotonin and noradrenaline reuptake inhibitors (SNRIs), benzodiazepines (BZDs), non-benzodiazepines GABA acting agent (No BZDs), acetylcholinesterase inhibitors (AChEIs), and N-methyl-D-aspartate receptors (NMDARs) was controlled. The ADMCI patients using those drugs could take their medications immediately after rsEEG experiments, planned in the late morning. Therefore, they just delayed the assumption of their medications for few hours than their normal routine. Table 2 reports information about the use of the above drug classes in ADMCI patients. Furthermore, Table 2 reports the number and the percentages of the ADMCI patients of the 1st, 2nd, and 3rd tertile assuming the above-mentioned drug classes. No statistically

Table 2
Number and percentages of ADMCI patients of the 1st (youngest age, $N = 21$), 2nd (median age, $N = 21$), and 3rd (oldest age, $N = 21$) tertile assuming the selective serotonin reuptake inhibitors (SSRIs), selective serotonin and noradrenaline reuptake inhibitors (SNRIs), benzodiazepines (BZDs), non-benzodiazepines GABA acting agent (No-BZDs), acetylcholinesterase inhibitors (AChEIs), and N-methyl-D-aspartate receptors (NMDARs). Type of drugs received by the ADMCI patients of the present study and the presence or absence of statistically significant differences (Freeman Halton test, $p < 0.05$ corrected) among the ADMCI tertiles are also reported. n.s., not significant ($p > 0.05$ corrected)

DRUGS	ADMCI 1st tertile *N* (%) Type	ADMCI 2nd tertile *N* (%) Type	ADMCI 3rd tertile *N* (%) Type	Freeman Halton test
Selective serotonin reuptake inhibitors (SSRIs)	6 (28.6%) Citalopram Sertraline	6 (28.6%) Citalopram Escitalopram	5(23.8%) Citalopram Escitalopram	n.s. n.s.
Selective serotonin and noradrenaline reuptake inhibitors (SNRIs)	1 (4.8%) Duloxetine	5 (23.8%) Duloxetine Venflaxine	1 (4.8%) Venflaxine	n.s.
Benzodiazepines (BZDs)	1 (4.8%) Alprazolam	1 (4.8%) Alprazolam	2 (9.5%) Alprazolam	n.s.
Non benzodiazepine GABA acting agents (No-BZDs)	0 (0%)	0 (0%)	0 (0%)	n.s.
Acetylcholinesterase inhibitors (AChEIs)	5 (23.8%) Donepezil Galantamine Rivastigmine	3 (14.3%) Donepezil	4 (19%) Donepezil	n.s.
N-methyl-D-aspartate receptors (NMDARs)	0 (0%)	0 (0%)	1 (4.8%)	n.s.
All drugs	9 (42.9%)	12 (57.1%)	11 (52.4%)	n.s.

significant difference was found among the ADMCI tertile in the use of the above medications even when a marginal threshold of $p < 0.05$ uncorrected was used.

The resting state electroencephalographic recordings

The rsEEG activity was recorded while the participants were relaxed with eyes closed and seated on a comfortable reclined chair in a silent room with dim lights. Instructions encouraged the participants to experience quiet wakefulness with muscle relaxation, no voluntary movements, no talking, and no development of systematic goal-oriented mentalization during the rsEEG recording. Rather, a quiet wondering mode of mentalization was kindly required. The participants, including the ADMCI patients, did not experience any significant difficulties following those instructions.

In all participants, the (eyes-closed) rsEEG recordings lasted about 3–5 min. Considering all clinical recording units, the rsEEG data were recorded with a sampling frequency of 128–512 Hz and related antialiasing bandpass between 0.01 Hz and 60–100 Hz. The electrode montage included 19 scalp monopolar sensors placed following the 10–20 System (i.e., O1, O2, P3, Pz, P4, T3, T5, T4, T6, C3, Cz, C4, F7, F3, Fz, F4, F8, Fp1, and Fp2; Fig. 1). A frontal ground electrode was used, while cephalic or linked earlobe electrodes were used as electric references according to local methodological facilities and

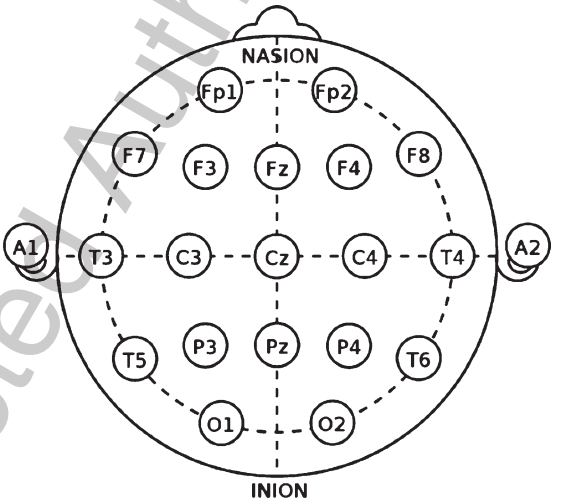

Fig. 1. Electroencephalographic (EEG) electrode montage. The electrode montage included 19 scalp monopolar sensors placed following the 10–20 System (i.e., O1, O2, P3, Pz, P4, T3, T5, T4, T6, C3, Cz, C4, F7, F3, Fz, F4, F8, Fp1, and Fp2).

standards. Electrode impedances were kept below 5 kΩ. Vertical and horizontal electro-oculographic (EOG) potentials (0.3–70 Hz bandpass) were recorded to control eye movements and blinking.

The preliminary rsEEG data analysis

The preliminary analysis of the recorded rsEEG activity followed the same procedures of previous rsEEG investigations performed in aMCI patients by

our Workgroup [56, 57] to compare the results across the various studies.

For this analysis, the rsEEG data were re-sampled to a sampling frequency of 128 Hz and divided into epochs of 2 s and analyzed offline. The rsEEG epochs affected by any physiological (ocular/blinking, muscular, cardiac, and head movements) or non-physiological (sweat, bad contact between electrodes and scalp, etc.) artifacts were identified and discarded by the visual analysis of two experts of EEG signals (C.D.P., G.N., S.L. or R.L.). In this visual analysis, the contamination of rsEEG rhythms with the ocular activity (i.e., blinking) was mainly evaluated in the frontal electrodes (i.e., F7, F3, Fz, F4, F8, Fp1, and Fp2), comparing the EOG and EEG traces. Head movement artefacts were detected based on their typical features, such as a sudden and great increase in amplitude in the form of very slow EEG waves in all scalp electrodes. Muscle tension artefacts were recognized by observing the effects of several frequency bandpass filters in different ranges and examining rsEEG power density spectra. These artefacts were reflected by unusually high and stable values of rsEEG power density from 30 to 100 Hz, which contrast with the typical declining trend of rsEEG power density from 25 Hz onward in artifact-free EEG traces. The experimenters also detected rsEEG epochs with signs of sleep intrusion (even if the rsEEG recordings lasted few minutes), such as progressive amplitude increase of frontal theta rhythms, followed by K complexes, sleep spindles, vertex shape waves, and slow waves. Furthermore, the two experimenters carefully rejected rsEEG epochs associated with behavioral annotations taken during the experiments (e.g., report of participant's drowsiness, opened eyes, arm/hand movements, or experimenter's verbal warnings, etc.).

As a result of the above procedures, the artifact-free epochs showed the same proportion of the total amount of rsEEG activity recorded in all Nold and ADMCI subgroups (>80%). In particular, the mean of artifact-free rsEEG epochs were 132 (±3 SE; 88.3%) in the Nold 1st tertile, 129 (±4 SE; 86.4%) in the Nold 2nd tertile, 132 (±3 SE; 88.0%) in the Nold 3rd tertile, 128 (±3 SE; 85.4%) in the ADMCI 1st tertile, 133 (±3 SE; 88.6%) in the ADMCI 2nd tertile, and 126 (±4 SE; 83.6%) in the ADMCI 3rd tertile. An ANOVA, including the factors Group (Nold and ADMCI) and Age (1st tertile, 2nd tertile, 3rd tertile), showed no statistically significant difference ($p > 0.05$) in the amount of the artifact-free rsEEG epochs between the two groups (Nold versus ADMCI) as well as the age tertiles (1st tertile versus 2nd tertile versus 3rd tertile). The mean lengthiness of the artifact-free rsEEG activity was >4 min for each group, ensuring the reliability of the rsEEG alpha power density [58, 59].

Scalp power density of rsEEG rhythms

For each ADMCI and Nold participant, the global normalized rsEEG power density at the scalp electrode level was evaluated. In detail, the procedure was performed as follows:

(1) A standard digital FFT-based power spectrum analysis (Welch technique, Hanning windowing function, no phase shift) computed the absolute scalp power density of rsEEG rhythms with 0.5 Hz of frequency resolution at each electrode (i.e., 19 electrodes of the 10–20 montage system) and frequency bin (i.e., 0.5–45 Hz) from all artifact-free rsEEG epochs.
(2) The scalp rsEEG power density at each electrode and frequency bin was normalized to the mean value obtained averaging the scalp rsEEG power density across all frequency bins and scalp electrodes.
(3) The "global" scalp normalized rsEEG power density at each frequency bin was calculated averaging the normalized scalp rsEEG power density values across all 19 electrodes of the 10–20 montage system.
(4) The global scalp normalized rsEEG power density values at each frequency band of interest were averaged to obtain the frequency band values. The rsEEG frequency bands of interest were individually identified based on the following frequency landmarks, namely the transition frequency (TF) and individual alpha frequency peak (IAFp) [4]. In the rsEEG power density spectrum, the TF marks the transition frequency between the theta and alpha bands, defined as the minimum of the rsEEG power density between 3 and 8 Hz (between the delta and the alpha power peak). The IAFp is defined as the maximum power density peak between 6 and 14 Hz. These frequency landmarks were previously well described by Dr. Wolfgang Klimesch [4, 60, 61]. The TF and IAFp were computed for each subject involved in the study. Based on the TF and IAFp, we estimated the individual delta, theta, and alpha

bands as follows: delta from TF –4 Hz to TF –2 Hz, theta from TF –2 Hz to TF, alpha 1 from TF to the frequency midpoint of the TF-IAFp range, alpha 2 from the frequency midpoint of the TF-IAFp range to IAFp, and alpha 3 IAFp to IAFp +2 Hz. The other bands were defined based on the standard fixed frequency ranges used in previous field studies of our Workgroup [56]: beta 1 from 14 to 20 Hz, beta 2 from 20 to 30 Hz, and gamma from 30 to 40 Hz.

Figure 2 shows two rsEEG epochs lasting 2 s each, one relative to a Nold participant and the other to an ADMCI patient. The rsEEG activity is plotted for all scalp electrodes. As an example of the general methodology, Fig. 2 also shows global EEG power density spectra averaged across all electrodes for these two rsEEG epochs.

The estimation of rsEEG cortical sources by low-resolution brain electromagnetic tomography (eLORETA) freeware

We used the official freeware tool called exact low-resolution brain electromagnetic tomography (eLORETA) for the linear estimation of the cortical source activity generating scalp-recorded rsEEG rhythms [62]. The present implementation of eLORETA uses a spherical head volume conductor model composed of the scalp, skull, and brain. In the scalp compartment, exploring electrodes can be virtually positioned to give EEG data as an input to the source estimation [62]. The brain model is based on a realistic cerebral shape taken from a template typically used in neuroimaging studies, namely that of the Montreal Neurological Institute (MNI152 template).

The input for eLORETA source estimation is artifact-free EEG epochs with 19 scalp electrodes, placed according to the 10–20 montage system. The output is the set of estimates of neural ionic currents in the brain source space formed by 6,239 voxels with 5 mm resolution, restricted to the cortical GM of the spherical head volume conductor model. In that cortical source space, an equivalent current dipole is in each voxel. For each voxel, the eLORETA package provides the Talairach coordinates, the cortical lobe, and the Brodmann area (BA).

The eLORETA freeware solves the so-called EEG inverse problem estimating "neural" current density values at any cortical voxel of the mentioned spherical head volume conductor model. The solutions are computed at all rsEEG frequency bin-by-frequency bin (0.5 Hz as frequency resolution, namely, the maximum frequency resolution allowed by the use of 2-s artifact-free EEG epochs).

In line with the general low spatial resolution of the present EEG methodological approach (i.e., 19 scalp electrodes), we performed a regional analysis of the eLORETA solutions. The following six lobar macroregions of interest (ROIs) were considered: frontal (Brodmann area, BA 8, 9, 10, 11, 44, 45, 46, and 47), central (BA 1, 2, 3, 4, and 6), parietal (BA 5, 7, 30, 39, 40, and 43), occipital (BA 17, 18, and 19), temporal (BA 20, 21, 22, 37, 38, 41, and 42), and limbic (BA 31, 32, 33, 34, 35, 36). Remarkably, the eLORETA solution for each lobar ROI was obtained by the average of the normalized eLORETA current density values estimated at all single voxels included in that ROI. For example, the eLORETA solution for the temporal ROI was obtained by the average of the normalized eLORETA current density values estimated at all voxels included in the BA 20, 21, 22, 37, 38, 41, and 42 of the bilateral temporal lobes. As a second example, the eLORETA solution for the occipital ROI was obtained by the same principle for the BA 17, 18, and 19 of the bilateral occipital lobes.

Statistical analyses

Two statistical sessions were performed by the commercial tool STATISTICA 10 (StatSoft Inc., http://www.statsoft.com) to test the main study hypotheses. In all statistical sessions, an ANOVA was computed using the global scalp normalized rsEEG power density or regional normalized eLORETA current density as a dependent variable ($p < 0.05$). In the ANOVA models, the complexity of the present ANOVA designs, including the factors Group X Age X Band X ROI (from 24 to 144 levels), basically considered the number of participants (N = 123).

It is well-known that the use of ANOVA models implies that dependent variables approximate Gaussian distributions, so we tested this feature in the global scalp normalized rsEEG power densities and regional normalized eLORETA current densities of interest by Kolmogorov-Smirnov test. The hypothesis of Gaussian distributions was tested at $p > 0.05$ (i.e., $p > 0.05$ = Gaussian, $p \leq 0.05$ = non-Gaussian). As the distributions of the global scalp normalized rsEEG power densities and regional normalized eLORETA current densities were not Gaussian in all cases, those variables underwent the log-10 transformation and re-tested. Such a transformation is a popular method to transform skewed

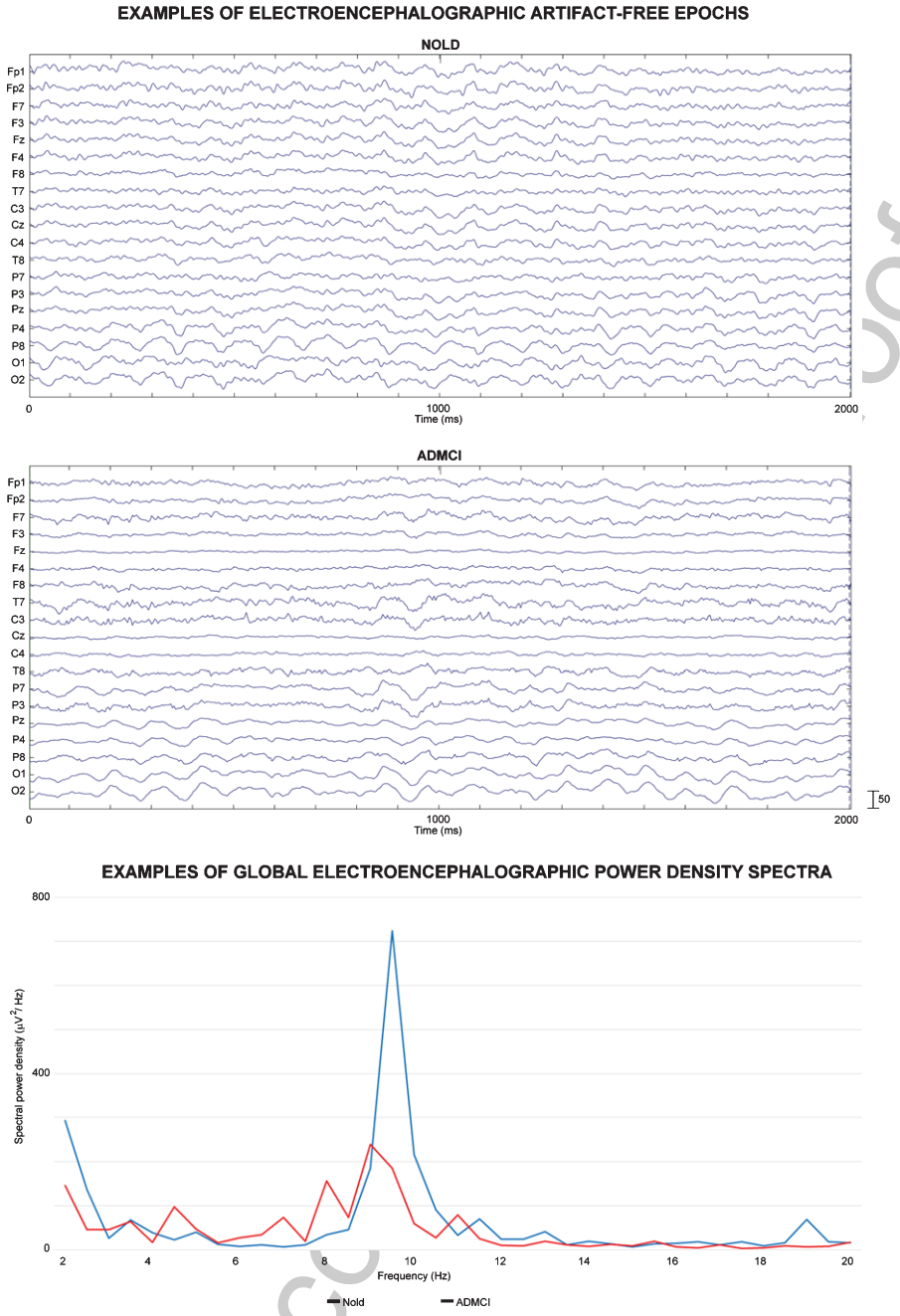

Fig. 2. Examples of artifact-free resting state eyes-closed electroencephalographic (rsEEG) epoch of 2 seconds in a healthy cognitively unimpaired (Nold) senior and a patient with Alzheimer's disease and mild cognitive impairment (ADMCI). The EEG traces of 19 scalp monopolar sensors (i.e., 10–20 System O1, O2, P3, Pz, P4, T3, T5, T4, T6, C3, Cz, C4, F7, F3, Fz, F4, F8, Fp1, and Fp2). For each of them, the figure also shows rsEEG power density spectra obtained averaging solutions at all scalp electrodes.

data distribution with all positive values (as global scalp normalized rsEEG power densities and regional normalized eLORETA current densities are) to Gaussian distributions, thus augmenting the reliability of the ANOVA results. Indeed, the outcome of the procedure approximated the distributions of all global scalp normalized rsEEG power densities and regional normalized eLORETA current densities to Gaussian distributions ($p > 0.05$ = Gaussian), allowing the use of the ANOVA model.

Mauchly's test evaluated the sphericity assumption, and degrees of freedom were corrected by the Greenhouse-Geisser procedure when appropriate ($p < 0.05$). Duncan test was used for *post-hoc* comparisons ($p < 0.05$, corrected for multiple comparisons as explained in the following).

The results of the following statistical analyses were controlled by the iterative (leave-one-out) Grubbs' test detecting for the presence of one or more outliers in the distribution of the global scalp normalized rsEEG power densities and regional normalized eLORETA current densities of interest. The null hypothesis of the non-outlier status was tested at the arbitrary threshold of $p > 0.001$ to remove only individual values with a high probability to be outliers.

In the first statistical session, an ANOVA evaluated the hypothesis that the global rsEEG scalp power density may be related to the aging in the Nold seniors and ADMCI patients. The ANOVA factors were Group (Nold and ADMCI), Age (1st tertile, 2nd tertile, 3rd tertile), and Band (delta, theta, alpha 2, and alpha 3). The TF, IAFp, and sites of the clinical units were used as covariates (these units contributed to the database with balanced percentages ranging from about 10% to 20%). The confirmation of the hypothesis would require: 1) a statistically significant ANOVA interaction including the factors Group and Band ($p < 0.05$) and 2) a *post-hoc* Duncan test indicating statistically significant ($p < 0.05$ Bonferroni corrected) differences in the global rsEEG scalp power density between the two Nold and ADMCI groups (i.e., between-group differences: Nold $\neq$ ADMCI, $p < 0.05$ Bonferroni corrected) and the age tertiles (i.e., within-group differences 1st tertile $\neq$ 2nd tertile $\neq$ 3rd tertile, $p < 0.05$ Bonferroni corrected).

The second statistical session probed the spatial features of the expected effects, with the low resolution and the exploratory mode allowed using only 19 scalp exploring electrodes (10–20 System). In this statistical session, an ANOVA evaluated the hypothesis that the rsEEG source activities (i.e., regional normalized eLORETA current densities) may be related to the aging in the Nold seniors and ADMCI patients. The ANOVA factors were Group (Nold and ADMCI), Age (1st tertile, 2nd tertile, 3rd tertile), Band (delta, theta, alpha 2, and alpha 3), and ROI (frontal, central, parietal, occipital, temporal, and limbic). The TF, IAFp and different clinical units were used as covariates. The confirmation of the hypothesis would require: 1) a statistically significant ANOVA interaction including the factors Group and Band ($p < 0.05$) and 2) a *post-hoc* Duncan test indicating statistically significant ($p < 0.05$ Bonferroni corrected) differences in the rsEEG source activities (i.e., regional normalized eLORETA current densities) between the two groups (i.e., between-group differences: Nold $\neq$ ADMCI, $p < 0.05$ Bonferroni corrected) and the age tertiles (i.e., within-group differences 1st tertile $\neq$ 2nd tertile $\neq$ 3rd tertile, $p < 0.05$ Bonferroni corrected).

RESULTS

Control markers in the ADMCI 1st tertile versus ADMCI 2nd tertile versus ADMCI 3rd tertile

Table 3 reports the most relevant clinical (i.e., GDS, CDR, and Hachinski Ischemic Score), genetic (i.e., *APOE4* genotyping), cerebrospinal fluid (i.e., $A\beta_{42}$, t-tau, p-tau, and $A\beta_{42}$/p-tau), anthropometric (i.e., weight, height, and body mass index), and cardiocirculatory (i.e., systolic pressure, diastolic pressure, pulse pressure, mean arterial pressure, and heart frequency) features in the ADMCI 1st tertile, ADMCI 2nd tertile, and ADMCI 3rd tertile. Table 3 also reports the results of the presence or absence of statistically significant differences ($p < 0.05$) among the ADMCI tertiles (i.e., ADMCI 1st tertile versus ADMCI 2nd tertile versus ADMCI 3rd tertile) for the above mentioned clinical (ANOVA), genetic (Chi-square test), cerebrospinal fluid (ANOVA), anthropometric (ANOVA), and cardiocirculatory (ANOVA) markers. To consider the inflating effects of repetitive univariate tests, the statistical threshold was set at $p < 0.003125$ one tail (i.e., 16 markers, $p < 0.05/16 = 0.003$) to obtain the Bonferroni correction at $p < 0.05$. Statistically significant differences were found neither considering that correction ($p > 0.003$) nor ignoring that correction ($p > 0.05$ uncorrected).

Table 4 reports the mean values ($\pm$ SE) of the following neuropsychological tests in the ADMCI 1st tertile, ADMCI 2nd tertile, and ADMCI 3rd tertile: ADAS-Cog, Rey Auditory Verbal Learning Test (immediate and delayed recall), TMT B-A, Verbal fluency for letters, Verbal fluency for category, Clock drawing, and Clock copy. Furthermore, Table 4 includes the cut-off (threshold) scores defining the abnormality of patients as measured by the above-mentioned neuropsychological tests [54, 63, 64] and the percentage of patients with abnormal scores for each tertile. For example, an ADAS-Cog score equal

Table 3
Mean values (± SE) of the clinical (i.e., Geriatric Depression Scale, Clinical Dementia Rating, and Hachinski Ischemic Score), genetic (i.e., Apolipoprotein E genotyping, *APOE*), cerebrospinal fluid (i.e., beta amyloid 1–42, $A\beta_{42}$; protein tau, t-tau; phosphorylated form of protein tau, p-tau; and $A\beta_{42}$/p-tau ratio), anthropometric (i.e., weight, height, and body mass index), and cardio-circulatory (i.e., systolic pressure, diastolic pressure, pulse pressure, mean arterial pressure, and heart frequency) variables as the results of their statistical comparisons ($p < 0.05$ corrected) in the ADMCI patients stratified according to the age in the youngest age tertile (ADMCI 1st tertile, $N = 21$), median age tertile (ADMCI 2nd tertile, $N = 21$), and oldest age tertile (ADMCI 3rd tertile, $N = 21$). In line with the inclusion criteria, all ADMCI patients had CDR score of 0.5, GDS score ≤ 5, and Hachinski Ischemic Score ≤ 4. n.s., not significant ($p > 0.05$ corrected)

Clinical, genetic (*APOE*), cerebrospinal fluid, anthropometric, and cardiocirculatory markers in ADMCI patients				
	ADMCI 1st tertile	ADMCI 2nd tertile	ADMCI 3rd tertile	Statistical analysis
Clinical markers				
Geriatric depression scale	2.6 ± 0.4 SE	2.6 ± 0.4 SE	2.5 ± 0.3 SE	ANOVA: n.s.
Clinical dementia rating	0.5 ± 0.0 SE	0.5 ± 0.0 SE	0.5 ± 0.0 SE	ANOVA: n.s.
Hachinski ischemic score	0.6 ± 0.2 SE	0.8 ± 0.1 SE	1.1 ± 0.2 SE	ANOVA: n.s.
Genetic marker				
Apolipoprotein E genotyping	0 ε2/ε3 3 ε3/ε3 1 ε2/ε4 13 ε3/ε4 4 ε4/ε4	1 ε2/ε3 4 ε3/ε3 1 ε2/ε4 11 ε3/ε4 4 ε4/ε4	1 ε2/ε3 6 ε3/ε3 0 ε2/ε4 14 ε3/ε4 0ε4/ε4	Chi-square test: n.s.
Cerebrospinal fluid markers (pg/mL)				
$A\beta_{42}$ (pg/ mL)	532 ± 31 SE	484 ± 28 SE	481 ± 28 SE	ANOVA: n.s.
p-tau (pg/mL)	82 ± 8 SE	89 ± 10 SE	86 ± 8 SE	ANOVA: n.s.
t-tau (pg/mL)	616 ± 83 SE	584 ± 75 SE	698 ± 116 SE	ANOVA: n.s.
$A\beta_{42}$/p-tau (pg/mL)	7.7 ± 0.8 SE	6.6 ± 0.7 SE	6.6 ± 0.8 SE	ANOVA: n.s.
Anthropometric markers				
Weight (kg)	67 ± 2 SE	70 ± 3 SE	72 ± 2 SE	ANOVA: n.s.
Height (mm)	165 ± 2 SE	166 ± 2 SE	168 ± 2 SE	ANOVA: n.s.
Body mass index (BMI)	24.4 ± 0.8 SE	25.2 ± 0.9 SE	25.8 ± 7 SE	ANOVA: n.s.
Cardiocirculatory markers				
Systolic pressure (mmHg)	134 ± 3 SE	136 ± 3 SE	135 ± 3 SE	ANOVA: n.s.
Diastolic pressure (mmHg)	76 ± 2 SE	79 ± 1 SE	79 ± 2 SE	ANOVA: n.s.
Pulse pressure (mmHg)	58 ± 3 SE	57 ± 3 SE	56 ± 3 SE	ANOVA: n.s.
Mean arterial pressure (MAP, mmHg)	95 ± 2 SE	98 ± 2 SE	97 ± 2 SE	ANOVA: n.s.

Table 4
Mean values (± SE) of the neuropsychological scores (i.e., ADAS-Cog, Rey Auditory Verbal Learning Test immediate recall, Rey Auditory Verbal Learning Test delayed recall, Trail Making Test part B-A, Verbal fluency for letters, Verbal fluency for category, Clock drawing, and Clock copy) as well as the results of their statistical comparisons (ANOVA on log-10 transformed data; $p < 0.05$ corrected) in the ADMCI patients stratified according to the age in the youngest age tertile (ADMCI 1st tertile, $N = 21$), median age tertile (ADMCI 2nd tertile, $N = 21$), and oldest age tertile (ADMCI 3rd tertile, $N = 21$). The cut-off scores of the neuropsychological tests are also reported. ADAS-Cog, Alzheimer's Disease Assessment Scale-Cognitive Subscale; RAVLT, Rey Auditory Verbal Learning Test; TMT B-A, Trail Making Test Part B-A; n.s., not significant ($p > 0.05$ corrected)

Neuropsychological markers in ADMCI patients					
	Cut-off of abnormality	ADMCI 1st tertile	ADMCI 2nd tertile	ADMCI 3rd tertile	ANOVA
		Mean ± SE (% subjects with abnormal score)	Mean ± SE (% subjects with abnormal score)	Mean ± SE (% subjects with abnormal score)	
ADAS-Cog	< 17	19.7 ± 1.5 SE (70.0%)	21.6 ± 1.5 SE (65.0%)	23.2 ± 2.0 SE (72.2%)	n.s.
RAVLT, immediate recall	< 28.53	29.0 ± 2.5 SE (42.9%)	30.0 ± 2.0 SE (52.4%)	28.0 ± 2.3 SE (52.4%)	n.s.
RAVLT, delayed recall	< 17	3.8 ± 0.6 SE (76.2%)	3.5 ± 0.6 SE (71.4%)	4.1 ± 0.8 SE (57.1%)	n.s.
Trail making test B-A	> 187	129 ± 17 SE (30%)	129 ± 13 SE (23.8%)	157 ± 17 SE (35.0%)	n.s.
Clock drawing	< 4.69	3.7 ± 0.3 SE (66.7%)	4.1 ± 0.3 SE (76.2%)	3.6 ± 0.3 SE (57.1%)	n.s.
Clock copy	> 3	4.4 ± 0.3 SE (71%)	4.7 ± 0.1 SE (95.2%)	4.6 ± 0.1 SE (90.5%)	n.s.
Letter fluency	< 17	34.2 ± 2.3 SE (4.8%)	33.4 ± 2.2 SE (4.8%)	29.8 ± 2.4 SE (9.5%)	n.s.
Letter category	< 25	32.6 ± 2.6 SE (30%)	37.9 ± 2.2 SE (0%)	27.1 ± 2.8 SE (47.6%)	n.s. ($F = 4.6$, $p < 0.05$, 2nd tertile > 3rd tertile)

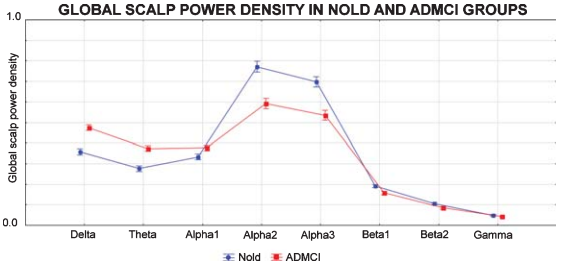

Fig. 3. Global scalp normalized power density values (mean across subjects, log-10 transformed) of rsEEG rhythms recorded in the groups of Nold ($N = 60$) and ADMCI patients ($N = 63$). Those values were computed for delta, theta, alpha 1, alpha 2, alpha 3, beta 1, beta 2, and gamma frequency bands.

to or lower than 17 is classified as "normal", whereas an ADAS-Cog score higher than 17 is usually considered to be "abnormal" (indicating a possible cognitive impairment); the percentage of patients with abnormal ADAS-Cog score (i.e., ADAS-Cog score higher than 17) was 70% for the ADMCI 1st tertile, 65% for the ADMCI 2nd tertile, and 72.2% for the ADMCI 3rd tertile. Table 4 also includes the results of the presence or absence of statistically significant differences (ANOVA; log-10 transformed data) among the ADMCI tertiles (i.e., ADMCI 1st tertile versus ADMCI 2nd tertile versus ADMCI 3rd tertile) for the neuropsychological tests used. To consider the inflating effects of repetitive univariate tests, the statistical threshold was set at $p < 0.00625$ (i.e., 8 neuropsychological tests, $p < 0.05/8 = 0.00625$) to obtain the Bonferroni correction at $p < 0.05$ one tail. No statistically significant differences were found considering that correction ($p > 0.00625$). Furthermore, a worsening of the Verbal fluency for category was found in the ADMCI 3rd tertile compared to the ADMCI 2nd tertile using an explorative statistical threshold of $p < 0.05$ uncorrected ($F = 4.6$, $p < 0.05$).

RsEEG scalp rhythms in the Nold versus ADMCI groups

Figure 3 shows the mean values (± SE, log-10 transformed) of rsEEG global scalp normalized power densities relative for two groups (Nold and ADMCI) and eight bands (delta, theta, alpha 1, alpha 2, alpha 3, beta 1, beta 2, and gamma). In the Nold group, the global scalp normalized power densities showed maximum magnitude at the alpha 2 and alpha 3 bands. Delta, theta, and alpha 1 global scalp normalized power densities showed a moderate magnitude when compared to that of alpha 2 and alpha 3 values.

Table 5
Mean values (± SE) of TF and IAFp computed from rsEEG power density spectra in the Nold seniors and ADMCI patients stratified according to the age in the youngest age tertile (Nold 1st tertile and ADMCI 1st tertile), median age tertile (Nold 2nd tertile and ADMCI 2nd tertile), and oldest age tertile (Nold 3rd tertile and ADMCI 3rd tertile)

Transition frequency (TF) and individual alpha frequency peak (IAFp) in Nold seniors and ADMCI patients			
	Nold 1st tertile	Nold 2nd tertile	Nold 3rd tertile
TF	5.9 ± 0.2 SE	6.1 ± 0.2 SE	6.2 ± 0.2 SE
IAFp	9.5 ± 0.2 SE	9.4 ± 0.2 SE	9.1 ± 0.2 SE
	ADMCI 1st tertile	ADMCI 2nd tertile	ADMCI 3rd tertile
TF	5.3 ± 0.3 SE	5.5 ± 0.3 SE	5.5 ± 0.2 SE
IAFp	8.2 ± 0.4 SE	8.4 ± 0.4 SE	8.7 ± 0.3 SE

Finally, beta 1, beta 2, and normalized power densities were characterized by lowest magnitude. As compared to the Nold group, the ADMCI group showed a substantial decrease in the global scalp normalized power densities at the alpha 2 and alpha 3 bands. Furthermore, the ADMCI group showed a substantial increase in the global scalp normalized power densities at the delta and theta bands in line with previous evidence in ADMCI and ADD patients [20, 21] and confirmed the selection of delta, theta, alpha 2, and alpha3 bands for the following statistical analyses.

TF and IAFp in the Nold and ADMCI tertiles

Table 5 reports the mean values of TF and IAFp for the Nold (i.e., Nold 1st tertile, Nold 2nd tertile, and Nold 3rd tertile) and ADMCI (i.e., ADMCI 1st tertile, ADMCI 2nd tertile, ADMCI 3rd tertile) tertiles. The TF mean was 5.9 Hz (± 0.2 SE) in the Nold 1st tertile, 6.1 Hz (± 0.2 SE) in the Nold 2nd tertile, 6.2 Hz (± 0.2 SE) in the Nold 3rd tertile, 5.3 Hz (± 0.3 SE) in the ADMCI 1st tertile, 5.5 Hz (± 0.3 SE) in the ADMCI 2nd tertile, and 5.5 Hz (± 0.2 SE) in the ADMCI 3rd tertile. Furthermore, the IAFp mean was 9.5 Hz (± 0.2 SE) in the Nold 1st tertile, 9.4 Hz (± 0.2 SE) in the Nold 2nd tertile, 9.1 Hz (± 0.2 SE) in the Nold 3rd tertile, 8.2 Hz (± 0.4 SE) in the ADMCI 1st tertile, 8.4 Hz (± 0.4 SE) in the ADMCI 2nd tertile, and 8.7 Hz (± 0.3 SE) in the ADMCI 3rd tertile.

Two ANOVAs ($p < 0.05$) were performed to evaluate the presence or absence of statistically significant differences ($p < 0.05$) among the two groups and the age tertiles for the TF and IAFp. The ANOVA factors were Group (Nold and ADMCI) and Age (1st tertile, 2nd tertile, 3rd tertile). Both ANOVAs showed

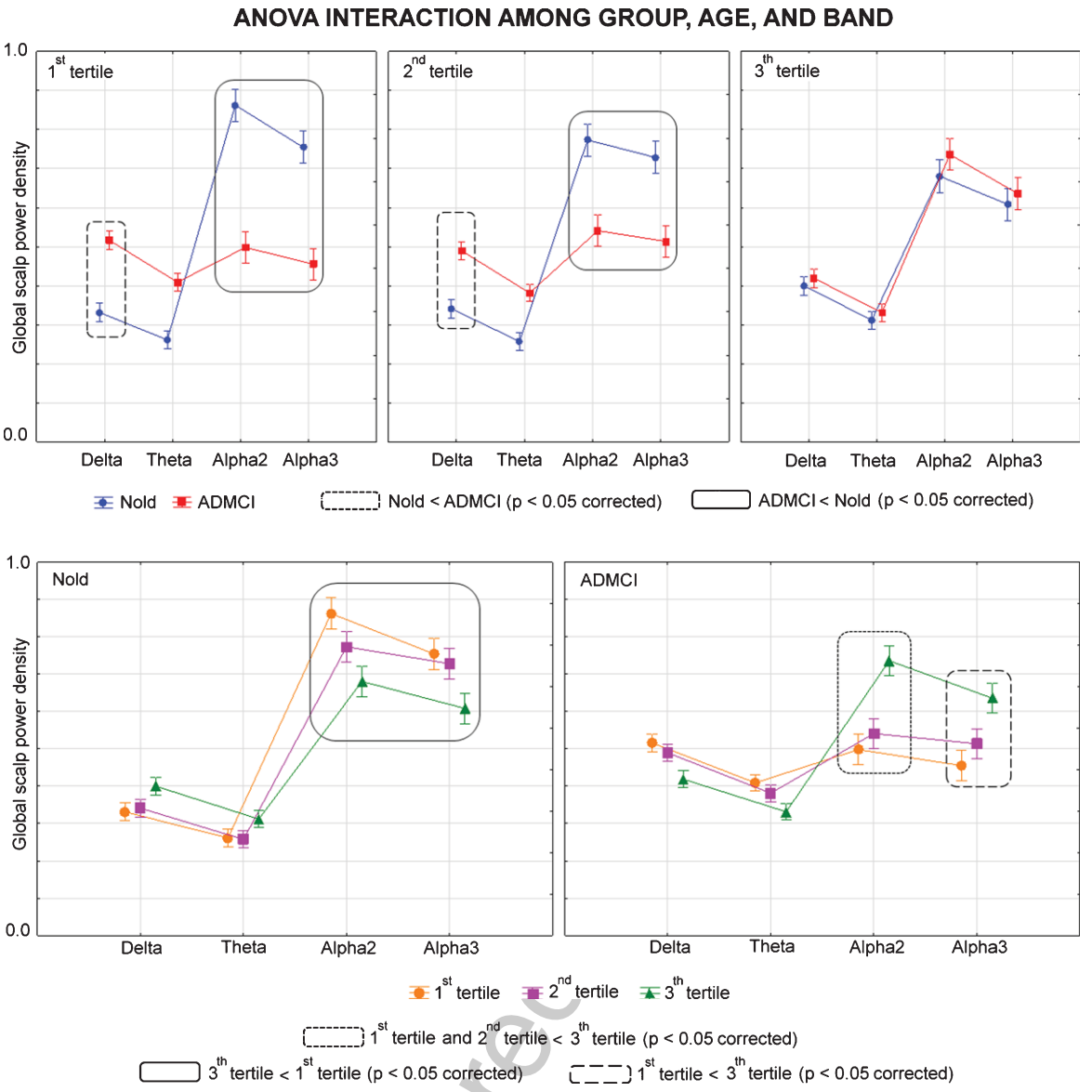

Fig. 4. Global scalp normalized rsEEG power density values (mean across subjects, log-10 transformed) about a statistical ANOVA interaction ($F = 12.4$, $p < 0.00001$) among the factors Group (Nold and ADMCI), Age (1st tertile, 2nd tertile, and 3rd tertile), and Band (delta, theta, alpha 2, and alpha 3). This ANOVA design used the global scalp normalized power densities as a dependent variable. The between-group (Nold versus ADMCI; *top figure*) and within-group (1st tertile versus 2nd tertile versus 3rd tertile*; bottom figure*) differences are illustrated. Legend: the rectangles indicate the frequency bands in which the global scalp normalized power densities statistically presented a significant difference among the two groups and the age tertiles ($p < 0.05$ corrected = $p < 0.002$).

a statistically significant main effect for the factor Group (TF: $F = 9.3$, $p < 0.005$; IAFp: $F = 13.3$, $p < 0.0005$), indicating that the TF and IAFp mean values were lower in the ADMCI than the Nold group.

These findings confirm that the alpha rhythms were slower in frequencies in the ADMCI group (about 6–10 Hz) than the Nold group (about 7–11 Hz). Therefore, the use of a fixed alpha frequency band at about 8–12 Hz would have penalized the cortical alpha source estimates in the ADMCI group.

RsEEG scalp rhythms in the Nold and ADMCI tertiles

Figure 4 shows the mean values (± SE, log-10 transformed) of the global rsEEG scalp normalized

Table 6
Size effect by Cohen's d as well as sample size by an alpha level of 0.05 and the desired power of 0.8 for the global scalp normalized power densities showing statistically significant ($p < 0.05$ corrected) between-group (Nold versus ADMCI) or within–group (1st tertile versus 2nd tertile versus 3rd tertile) differences

	Global scalp normalized power density	Size effect	Sample size
Nold 1st tertile versus	Delta	–1.70	7
ADMCI 1st tertile	Alpha 2	2.35	4
	Alpha 3	1.84	6
Nold 2nd tertile versus	Delta	–1.26	11
ADMCI 2nd tertile	Alpha 2	1.21	12
	Alpha 3	1.12	14
Nold 1st tertile versus	Alpha 2	1.29	11
Nold 3rd tertile	Alpha 3	1.15	13
ADMCI 1st tertile versus	Alpha 2	–1.17	13
ADMCI 3rd tertile	Alpha 3	–0.86	23
ADMCI 2nd tertile versus ADMCI 3rd tertile	Alpha 2	–0.88	22

power density relative to a statistically significant ANOVA interaction effect ($F = 12.4$, $p < 0.00001$) among the factors Group (Nold and ADMCI), Age (1st tertile, 2nd tertile, 3rd tertile), and Band (delta, theta, alpha 2, and alpha 3).

The Fig. 4 (top) illustrates the between-group differences (Nold versus ADMCI). The Duncan planned *post-hoc* ($p < 0.05$ Bonferroni correction for 2 groups X 3 age X 4 frequency bands, $p < 0.05/24 = 0.002$) testing showed that: 1) for the 1st tertile and 2nd tertile, the discriminant pattern Nold < ADMCI was fitted by the delta ($p < 0.001$) global scalp normalized power densities; and 2) for the 1st tertile and 2nd tertile, the discriminant pattern Nold > ADMCI was fitted by the alpha 2 ($p < 0.00001$) and alpha 3 ($p < 0.00001$) global scalp normalized power densities. No statistically significant between-group differences were observed for the 3rd tertile ($p > 0.002$).

The Fig. 4 (bottom) illustrates the within-group differences (1st tertile versus 2nd tertile versus 3rd tertile). The Duncan planned *post-hoc* ($p < 0.05$ corrected $= p < 0.002$) showed that: 1) for the Nold group, the discriminant pattern 1st tertile > 3rd tertile was fitted by the alpha 2 ($p < 0.0001$) and alpha 3 ($p < 0.002$) global scalp normalized power densities; and 2) for the ADMCI group, the discriminant pattern 1st tertile and 2nd tertile < 3rd tertile was fitted by the alpha 2 ($p < 0.00005$) global scalp normalized power densities; 3) for the ADMCI group, the discriminant pattern 1st tertile < 3rd tertile was fitted by the alpha 2 ($p < 0.0001$) global scalp normalized power densities.

Table 6 reports the size effect by Cohen's d and sample size by an alpha level of 0.05 and the desired power of 0.8 for the global scalp normalized power densities showing statistically significant ($p < 0.05$ corrected $= p < 0.002$) between-group (Nold versus ADMCI) or within-group (1st tertile versus 2nd tertile versus 3rd tertile) differences. The sample sizes ranged from 4 to 23, in line with the number of participants in the present Nold and ADMCI groups.

Of note, the above findings were not due to outliers from those individual global scalp normalized power densities (log-10 transformed), as shown by Grubbs' test with an arbitrary threshold of $p > 0.001$ (see Fig. 5).

RsEEG source activities in the Nold and ADMCI tertiles

Figure 6 shows the mean values (± SE, log-10 transformed) of rsEEG source activities (i.e., regional normalized eLORETA current densities) relative to a statistically significant ANOVA interaction effect ($F = 6.5$ $p < 0.0001$) among the factors Group (Nold and ADMCI), Age (1st tertile, 2nd tertile, 3rd tertile), Band (delta, theta, alpha 2, and alpha 3), and ROI (frontal, central, parietal, occipital, temporal, and limbic).

The Fig. 6 (top) illustrates the between-group differences (Nold versus ADMCI). The Duncan planned *post-hoc* ($p < 0.05$ Bonferroni correction for 2 groups X 3 age X 4 frequency bands X 6 ROIs, $p < 0.05/144 = 0.000347$) testing showed that: () for the 1st tertile, the discriminant pattern Nold < ADMCI was fitted by the frontal ($p < 0.00001$), occipital ($p < 0.0005$), and temporal ($p < 0.00001$) delta source activities; 2) for the 1st tertile, the discriminant pattern Nold > ADMCI was fitted by the central ($p < 0.0001$), parietal ($p < 0.00001$), occipital ($p < 0.00001$), temporal ($p < 0.00001$), and limbic ($p < 0.00001$) alpha 2 source activities as well as the central ($p < 0.0001$), parietal ($p < 0.00001$), occipital ($p < 0.00001$), temporal ($p < 0.00001$), and limbic ($p < 0.00001$) alpha 3 source activities; 3) for the 2nd tertile, the discriminant pattern Nold > ADMCI was fitted by the parietal ($p < 0.00001$), occipital ($p < 0.00001$), and limbic ($p < 0.0001$) alpha 2 source activities as well as the parietal ($p < 0.00001$), occipital ($p < 0.00001$), and limbic ($p < 0.0001$) alpha 3 source activities.

The Fig. 6 (bottom) illustrates the within-group differences (1st tertile versus 2nd tertile versus 3rd tertile). The Duncan planned *post-hoc* ($p < 0.05$ corrected $= p < 0.000347$) showed that: 1) for the Nold group, the discriminant pattern 1st tertile and 2nd

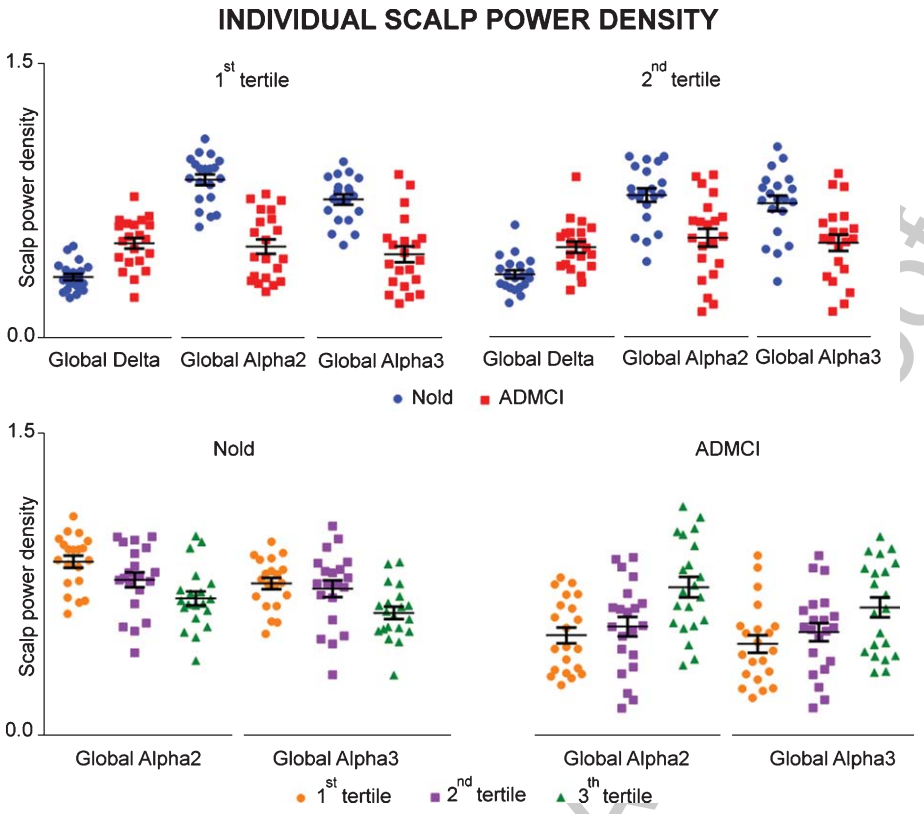

Fig. 5. Individual values (log-10 transformed) of the global scalp normalized rsEEG power densities showing statistically significant ($p < 0.05$ corrected = $p < 0.002$) between-group (Nold versus ADMCI) and within-group (1st tertile versus 2nd tertile versus 3rd tertile) differences.

tertile > 3rd tertile was fitted by the occipital alpha 2 ($p < 0.00001$) and alpha 3 ($p < 0.00001$) source activities; 2) the discriminant pattern 1st tertile > 3rd tertile was fitted by the parietal ($p < 0.00001$) and temporal ($p < 0.00001$) alpha 2 source activities as well as parietal ($p < 0.0001$) alpha 3 source activities; 3) for the ADMCI group, the discriminant pattern 1st tertile and 2nd tertile < 3rd tertile was fitted by the occipital ($p < 0.00001$) and temporal ($p < 0.00001$) alpha 2 source activities.

Table 7 reports the size effect by Cohen's d as well as the sample size by an alpha level of 0.05 and the desired power of 0.8 for the rsEEG source activities (i.e., regional normalized eLORETA current densities) showing statistically significant ($p < 0.05$ corrected = $p < 0.000347$) between-group (Nold versus ADMCI) or within-group (1st tertile versus 2nd tertile versus 3rd tertile) differences.

Of note, these findings were not due to outliers from those individual regional normalized eLORETA current densities (log-10 transformed), as shown by Grubbs' test with an arbitrary threshold of $p > 0.001$ (see Fig. 7).

Results of the control analyses

A first control analysis ($p < 0.05$ corrected) was performed to evaluate whether the above-described relationships between the rsEEG scalp variables and aging in the Nold seniors and the ADMCI patients may also be observed using standardized fixed delta, theta, and alpha frequency bands. To address this issue, the procedure was performed as follows: 1) for each Nold and ADMCI subjects, the global scalp normalized rsEEG power density values at each fixed frequency band of interest were averaged to obtain the frequency band values. The rsEEG fixed frequency bands of interest were delta from 2 to 4 Hz, theta from 4 to 8 Hz, low-frequency alpha from 8 to 10.5 Hz, and high-frequency alpha from 10.5 to 13 Hz; 2) For each fixed frequency band of interest, the rsEEG source activities (i.e., regional normalized eLORETA solutions) were log 10 transformed to make them Gaussian before the subsequent parametric statistical analysis; 3) An ANOVA was computed having the global scalp normalized rsEEG power density

as a dependent variable ($p < 0.05$). The ANOVA factors were Group (Nold and ADMCI), Age (1st tertile, 2nd tertile, 3rd tertile), and Band (delta, theta, low-frequency alpha, and high-frequency alpha). The different clinical units were used as a covariate. The results showed a statistically significant interaction effect ($F = 5.5$; $p < 0.0001$; see Fig. 8) among the three factors. Figure 8 (top) illustrates the between-group differences (Nold versus ADMCI). The Duncan planned *post-hoc* ($p < 0.05$ Bonferroni correction for 2 groups X 3 age X 4 frequency bands, $p < 0.05/24 = 0.002$) testing showed that for

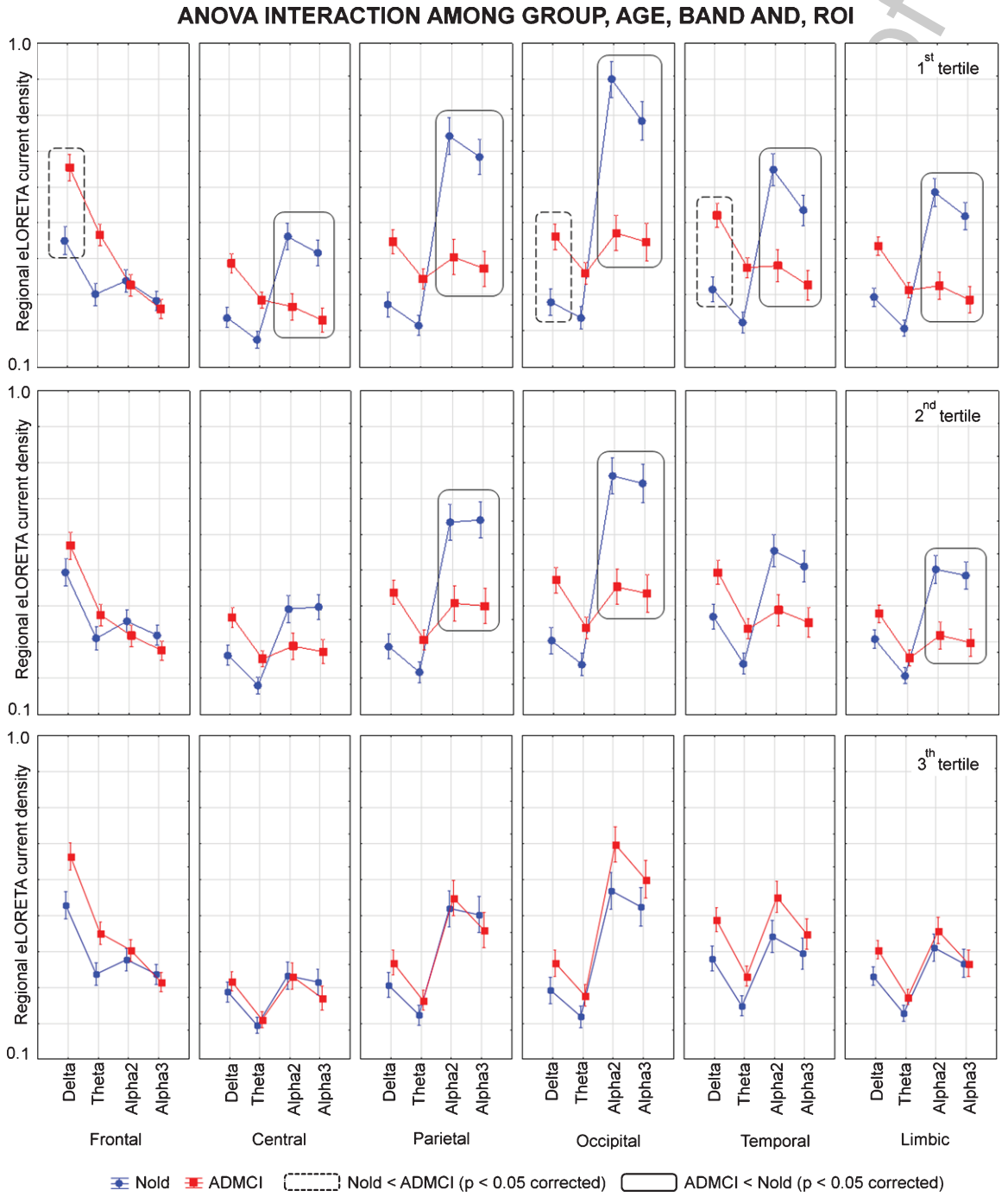

Fig. 6. *(Continued)*

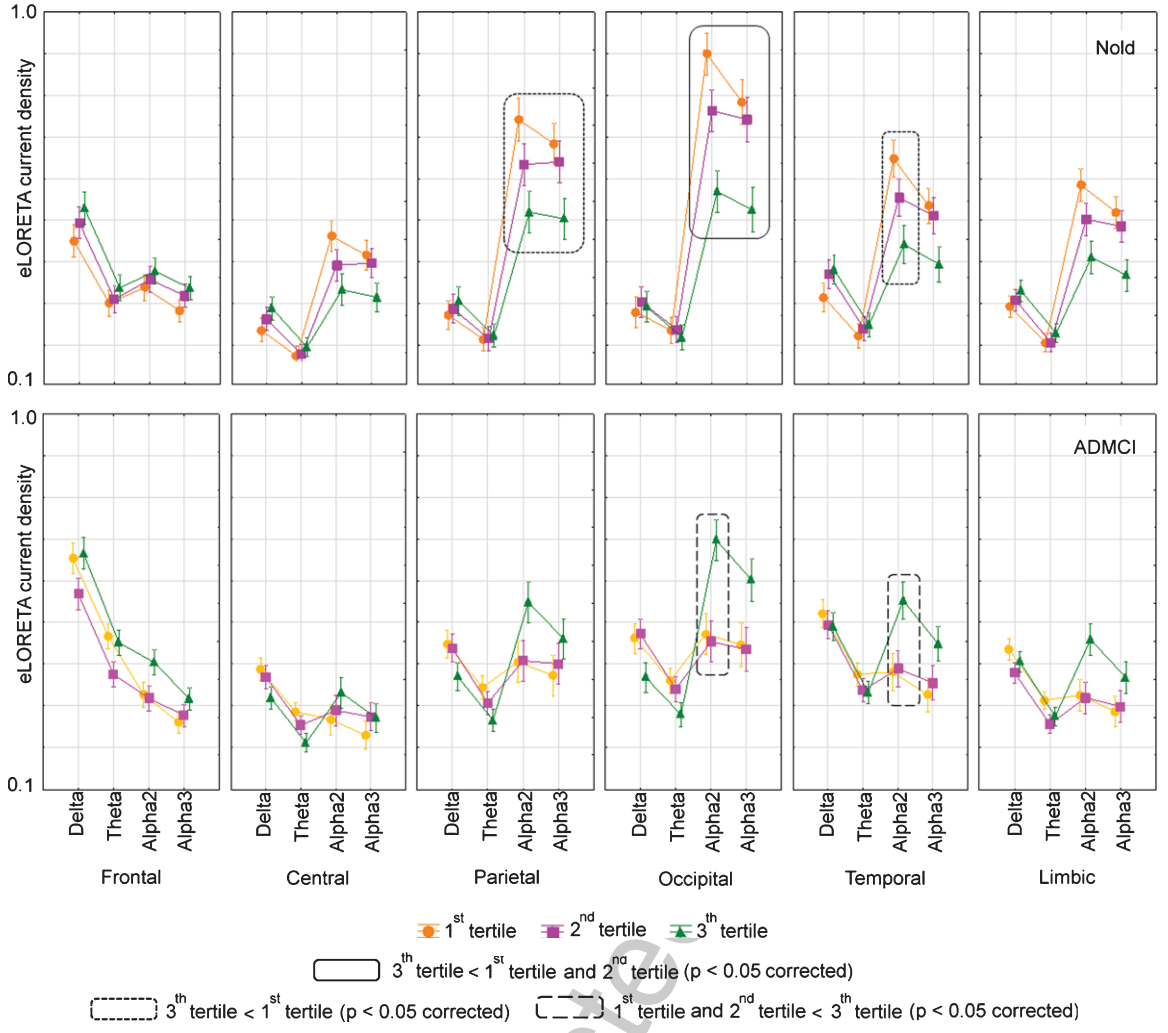

Fig. 6. Regional normalized exact low-resolution brain electromagnetic source tomography (eLORETA) solutions (mean across subjects, log-10 transformed) modeling cortical sources of eyes-closed rsEEG rhythms relative to a statistical ANOVA interaction ($F = 6.5$ $p < 0.0001$) among the factors Group (Nold and ADMCI), Age (1st tertile, 2nd tertile, and 3rd tertile), Band (delta, theta, alpha 2, and alpha 3), and Region of interest, ROI (central, frontal, parietal, occipital, temporal, and limbic). This ANOVA design used the regional normalized eLORETA solutions as a dependent variable. The between-group (Nold versus ADMCI; *top figure*) and within-group (1st tertile versus 2nd tertile versus 3rd tertile*; bottom figure*) differences are illustrated. Legend: the rectangles indicate the cortical regions and frequency bands in which the eLORETA solutions statistically presented a significant difference among the two groups and the age tertiles ($p < 0.05$ corrected = $p < 0.00035$).

the 1st tertile and 2nd tertile, the discriminant pattern Nold > ADMCI was fitted by the low-frequency alpha global scalp normalized power densities ($p < 0.0001$). No statistically significant between-group differences were observed for the 3rd tertile ($p > 0.002$). Figure 8 (bottom) illustrates the within-group differences (1st tertile versus 2nd tertile versus 3rd tertile). The Duncan planned *post-hoc* ($p < 0.002$) showed that: (i) for the Nold group, the discriminant pattern 1st tertile > 3rd tertile was fitted by the low-frequency global scalp normalized power densities ($p < 0.0005$); for the ADMCI group, the discriminant pattern 1st tertile < 3rd tertile was fitted by the low-frequency global scalp normalized power densities ($p < 0.0005$). Of note, these findings were not due to outliers from those individual global scalp normalized power densities (log-10 transformed), as shown by Grubbs' test with an arbitrary threshold of $p > 0.001$. Overall, the results of the first control analysis with fixed rsEEG frequency bands confirmed most of the age-related effects on the global rsEEG power density in the Nold and ADMCI

Table 7
Size effect by Cohen's d as well as sample size by an alpha level of 0.05 and the desired power of 0.8 for the rsEEG source activities (i.e., regional normalized eLORETA current densities) showing statistically significant ($p < 0.05$ corrected) between-group (Nold versus ADMCI) or within-group (1st tertile versus 2nd tertile versus 3rd tertile) differences

	Normalized eLORETA current density	Size effect	Sample size
Nold 1st tertile versus ADMCI 1st tertile	Frontal delta	–1.43	9
	Occipital delta	–1.06	16
	Temporal delta	–1.53	8
	Central alpha 2	1.14	14
	Parietal alpha 2	1.54	8
	Occipital alpha 2	1.91	6
	Temporal alpha 2	1.31	10
	Limbic alpha 2	1.54	8
	Central alpha 3	1.21	12
	Parietal alpha 3	1.37	10
	Occipital alpha 3	1.32	11
	Temporal alpha 3	1.12	14
	Limbic alpha 3	1.35	10
Nold 2nd tertile versus ADMCI 2nd tertile	Parietal alpha 2	1.13	14
	Occipital alpha 2	1.44	9
	Limbic alpha 2	1.22	12
	Parietal alpha 3	1.14	14
	Occipital alpha 3	*1.30*	11
	Limbic alpha 3	1.21	12
Nold 1st tertile versus Nold 3rd tertile	Parietal alpha 2	1.02	17
	Occipital alpha 2	1.84	6
	Temporal alpha 2	1.10	15
	Parietal alpha 3	0.77	28
	Occipital alpha 3	1.22	12
Nold 2nd tertile versus Nold 3rd tertile	Occipital alpha 2	0.96	19
	Occipital alpha 3	1.04	16
ADMCI 1st tertile versus ADMCI 3rd tertile	Occipital alpha 2	–0.88	22
	Temporal alpha 2	–0.78	27
ADMCI 2nd tertile versus ADMCI 3rd tertile	Occipital alpha 2	–1.06	16
	Temporal alpha 2	–0.78	27

groups observed using the individual rsEEG frequency bands.

A second control analysis ($p < 0.05$ corrected) was performed to confirm that the above differences among ADMCI tertiles in the rsEEG scalp and eLORETA source variables may be not due to 1) the global neurodegeneration of the cerebral cortex; 2) the neurodegeneration of particular cerebral structures as the mesial temporal cortex, basal ganglia, and lateral ventricle; and 3) cerebrovascular lesions. In that control analysis, we evaluated whether the MRI markers reflecting those pathological brain processes may differ among ADMCI 1st tertile, ADMCI 2nd tertile, and ADMCI 3rd tertile ($p < 0.05$ corrected for multiple comparisons as explained in the following).

For each ADMCI patient, the procedure was performed as follows: 1) the MRI markers included (i) the total GM and WM volumes (normalized with the total intracranial volume) and the total cortical thickness; (ii) the volumes of caudate, putamen, pallidum, accumbens, hippocampus, amygdala, and lateral ventricle (normalized with the total intracranial volume), and the thicknesses of the entorhinal cortex; and (iii) the WM hypointensity and WM lesions (see Table 8); 2) these MRI markers were log-10 transformed to make them Gaussian before the subsequent parametric statistical analysis; 3) ANOVAs were computed to evaluate the presence or absence of statistically significant differences among ADMCI tertiles for the above-mentioned MRI markers. To consider the inflating effects of multiple univariate tests, the statistical threshold was set at $p < 0.0038$ (i.e., 13 MRI markers, $p < 0.05/13 = 0.0038$) to obtain the Bonferroni correction at $p < 0.05$ on tail. No statistically significant differences were found considering the Bonferroni correction ($p > 0.0038 = 0.05$ corrected). Using an explorative statistical threshold of $p < 0.05$ uncorrected, a decrease in the total GM volume and total cortical thickness as well as an increase in the WM hypointensity were found in the ADMCI 3rd tertile as compared to the ADMCI 2nd tertile and ADMCI 1sr tertile (total GM volume: $F = 3.2$, $p < 0.05$; total cortical thickness: $F = 4.3$, $p < 0.05$; WM hypointensity: $F = 5.5$, $p < 0.01$). Figure 9 plots the individual values, the group means, and the SE of the total GM volume, the total cortical thickness, and the WM hypointensity in the three subgroups of the ADMCI patients (1sr, 2nd, and 3rd tertiles).

To further confirm that the above differences in the global rsEEG scalp power density among the ADMCI tertiles may be not due to the global neurodegeneration of the cerebral cortex and cerebrovascular lesions, we also performed a third control analysis. In that control analysis, we implemented the following procedure: 1) the enrolled ADMCI patients were stratified into two subgroups, respectively, based on the low and high normalized total GM volume (GM- and GM+), normalized WM volume (WM- and WM+), cortical thickness (THICK- and THICK+), and WM hypointensity (WM-Hypo- and WM- Hypo+); 2) Four ANOVAs were computed having the global scalp normalized rsEEG power density as a dependent variable ($p < 0.05$). The ANOVA factors were MRI level (GM- and GM+; WM- and WM+; THICK- and THICK+; WM-Hypo- and WM-Hypo+), Age (1st tertile, 2nd tertile, 3rd tertile), and Band (delta, theta, alpha 2, and alpha 3). Education,

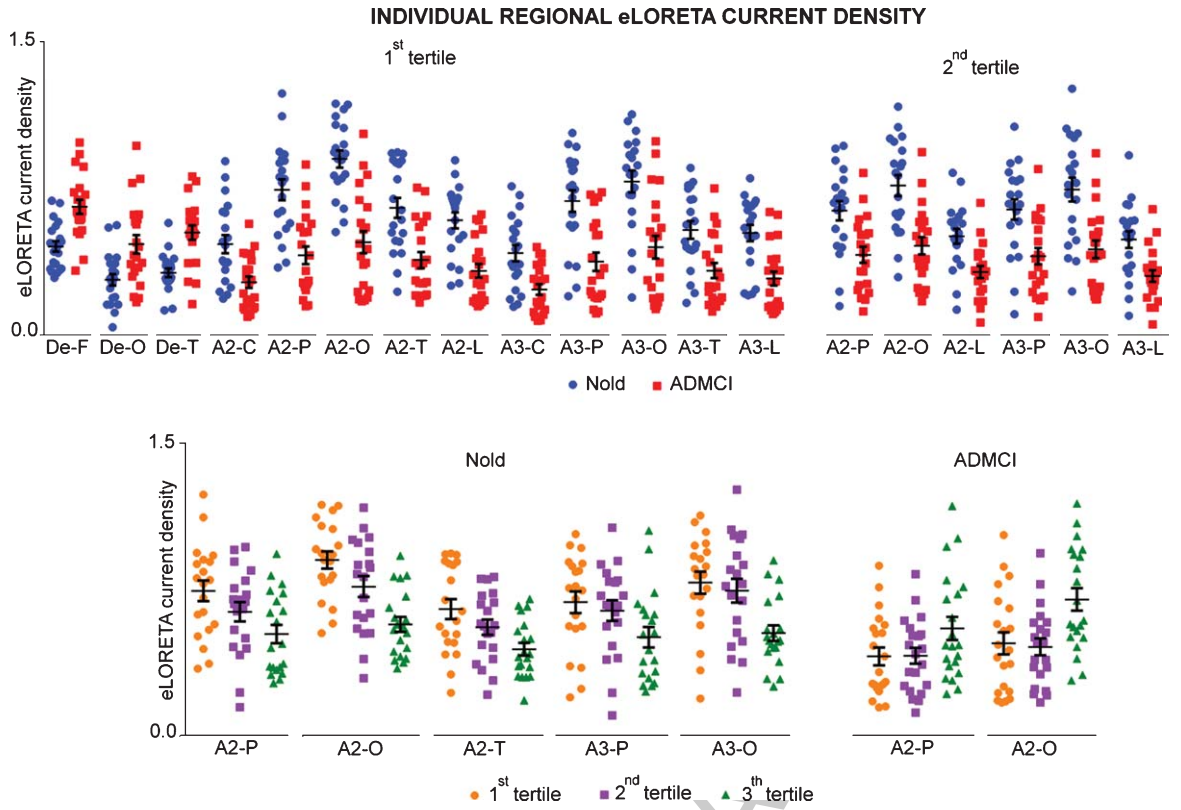

Fig. 7. Individual values (log-10 transformed) of the regional normalized eLORETA solutions showing statistically significant ($p < 0.05$ corrected = $p < 0.0003$) between-group (Nold versus ADMCI) and within-group (1st tertile versus 2nd tertile versus 3rd tertile) differences.

gender, MMSE score, TF, IAFp, and different clinical units were used as covariates. No statistically significant main effect for the factor MRI level or statistically significant interaction, including the factor MRI level, were found ($p > 0.05$).

Overall, the results of the second and third control analyses suggest that the age-related effects on the global rsEEG scalp power density and source activities among the ADMCI tertiles may be not substantially due to the neurodegeneration of cortical structures or cerebrovascular lesions.

A fourth control analysis was implemented by an independent statistical approach ($p < 0.05$ corrected) to "cross-validate" the results of the main statistical analysis. This control analysis tested the association between the age and the global rsEEG alpha 2 and 3 scalp normalized power density in the Nold and ADMCI groups. Given the complexity of the ANOVA models of the main analysis, it served to give robustness to the main findings and conclusions.

To the aim of the fourth control analysis, several linear regression models were computed. Specifically, the Age variable was considered as both categorical (e.g., ADMCI 1st tertile, ADMCI 2nd tertile, ADMCI 3rd tertile) and continuous to serve as a predictor, while the global rsEEG alpha 2 and 3 scalp normalized power density (one model for each variable) served as target variables. Also, the effect of *APOE4* was evaluated only in ADMCI patients. In these patients, the control statistical models considered the interaction between the Age variable as categorical (ADMCI 1st tertile, ADMCI 2nd tertile, ADMCI 3rd tertile) and the presence of *APOE4* (dichotomized in *APOE4* and *APOnonE4*) as a predictor and the global rsEEG alpha 2 and 3 scalp normalized power densities as target variables. Overall, the results of the fourth control analysis confirmed the findings of the main analysis. There were statistically significant effects of the Age (both categorical and continuous) on the global rsEEG alpha 2 and 3 scalp normalized power density in both Nold and ADMCI groups ($p < 0.05$). Notably, no effect of the interaction between Age and *APOE4* was observed in the ADMCI patients ($p > 0.05$). Beta coefficients of the model estimates, together with the relative statistics, are also reported in Table 9.

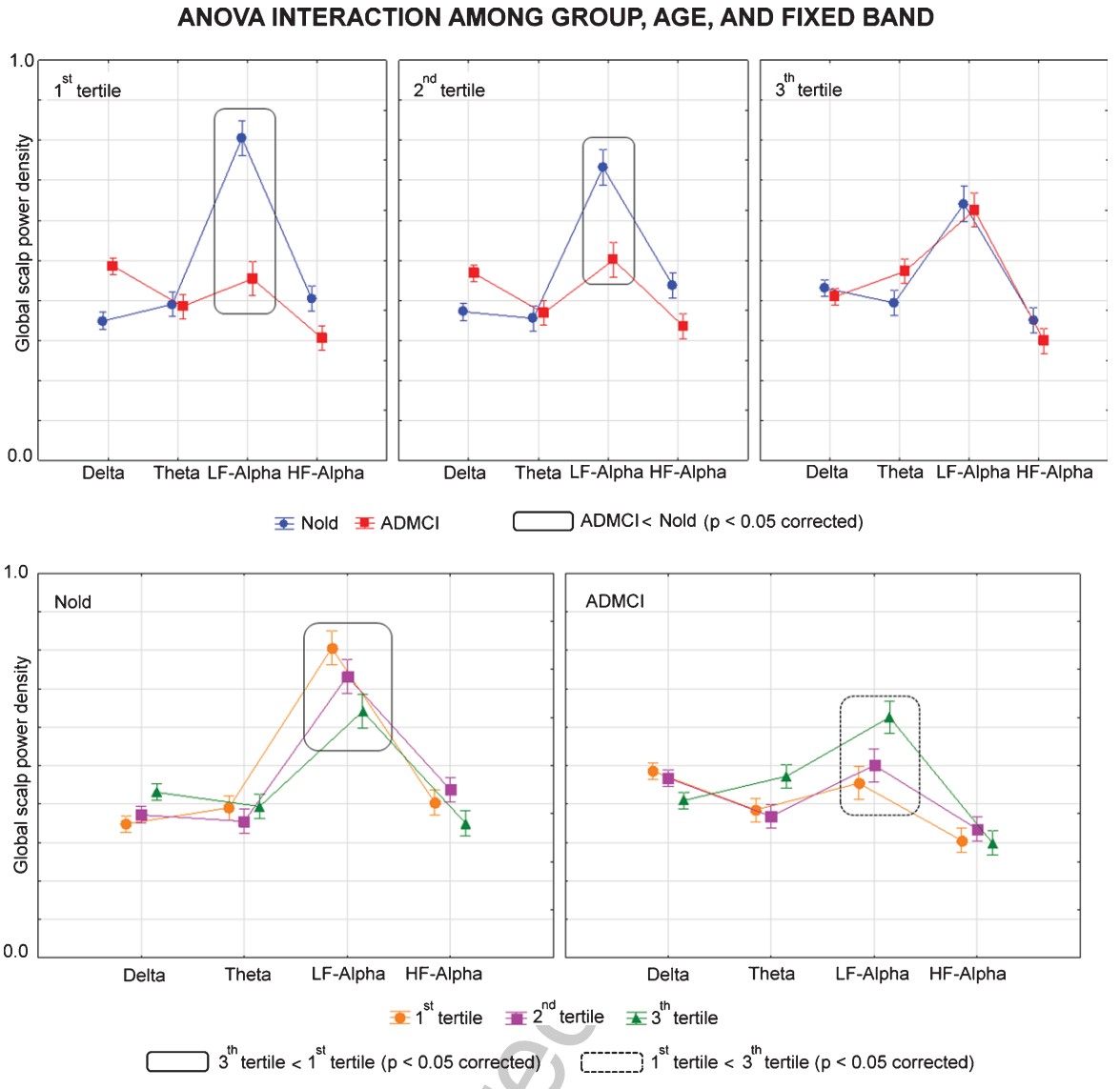

Fig. 8. Global scalp normalized rsEEG power density values (mean across subjects, log-10 transformed) about a statistical ANOVA interaction ($F = 5.5$, $p < 0.0001$) among the factors Group (Nold and ADMCI), Age (1st tertile, 2nd tertile, and 3rd tertile), and Fixed Band (delta, theta, low-frequency alpha, and high-frequency alpha). This ANOVA design used the global scalp normalized power densities as a dependent variable. The between-group (Nold versus ADMCI; *top figure*) and within-group (1st tertile versus 2nd tertile versus 3rd tertile*; bottom figure*) differences are illustrated. Legend: the rectangles indicate the frequency bands in which the global scalp normalized power densities statistically presented a significant difference among the two groups and the age tertiles ($p < 0.05$ corrected = $p < 0.002$).

DISCUSSION

In the present retrospective and exploratory study, we investigated whether the age factor may show similar progressive deranging effects on rsEEG rhythms in Nold and ADMCI seniors. The novel and original results are discussed in the following sections.

Progressive derangement of rsEEG alpha rhythms with age in Nold seniors

Concerning the physiological aging, the results of the main analysis showed that in the Nold group, the age factor did affect neither the TF nor the IAFp, which are the most robust individual benchmarks reflecting the slowing in frequency over the age of

Table 8
Mean values (± SE) of the magnetic resonance imaging (MRI) markers (i.e., volumes of the total gray matter, total white matter, caudate, putamen, pallidum, accumbens, hippocampus, amygdala, and lateral ventricle; cortical thicknesses of the total and entorhinal cortex; white matter hypointensity and lesions) as well as the results of their statistical comparisons (ANOVA on log-10 transformed data; $p < 0.05$ corrected) in the ADMCI patients stratified according to the age in the youngest age tertile (ADMCI 1st tertile, $N = 21$), median age tertile (ADMCI 2nd tertile, $N = 21$), and oldest age tertile (ADMCI 3rd tertile, $N = 21$). The volumes were normalized with reference to the total intracranial volume. n.s., not significant ($p > 0.05$ corrected)

MRI markers in ADMCI patients				
	ADMCI 1st tertile	ADMCI 2nd tertile	ADMCI 3rd tertile	ANOVA
Global markers				
Normalized WM volume	0.30 ± 0.01 SE	0.30 ± 0.01 SE	0.29 ± 0.01 SE	n.s.
Normalized GM volume	0.39 ± 0.01 SE	0.39 ± 0.01 SE	0.37 ± 0.01 SE	ANOVA: n.s. ($F = 3.2$, $p < 0.05$)
Cortical thickness	4.7 ± 0.05 SE	4.8 ± 0.05 SE	4.6 ± 0.06 SE	n.s. ($F = 4.3$, $p < 0.01$)
Basal ganglia markers				
Normalized caudate volume	0.004 ± 0.001 SE	0.004 ± 0.001 SE	0.005 ± 0.001 SE	n.s.
Normalized putamen volume	0.006 ± 0.001 SE	0.006 ± 0.001 SE	0.006 ± 0.001 SE	n.s.
Normalized pallidum volume	0.003 ± 0.001 SE	0.002 ± 0.001 SE	0.002 ± 0.001 SE	n.s.
Normalized accumbens volume	0.0006 ± 0.0001 SE	0.0006 ± 0.0001 SE	0.0005 ± 0.0001 SE	n.s.
Mesial temporal markers				
Normalized hippocampus volume	0.005 ± 0.001 SE	0.005 ± 0.001 SE	0.005 ± 0.001 SE	n.s.
Normalized amygdale volume	0.002 ± 0.001 SE	0.002 ± 0.001 SE	0.002 ± 0.001 SE	n.s.
Entorhinal cortical thickness	6.7 ± 0.1 SE	6.6 ± 0.1 SE	6.1 ± 0.1 SE	n.s.
Ventricular markers				
Normalized lateral ventricle volume	0.019 ± 0.001 SE	0.019 ± 0.001 SE	0.024 ± 0.001 SE	n.s.
Hypointensity/lesion WM markers				
WM hypointensity	2,022 ± 251 SE	2,364 ± 329 SE	3,907 ± 507 SE	n.s.
WM lesions	1,647 ± 419 SE	2,273 ± 631 SE	4,691 ± 1257 SE	n.s. ($F = 5.5$, $p < 0.005$)

the background rsEEG rhythms [4]. In contrast, the age factor affected the magnitude of rsEEG rhythms in the Nold seniors. As compared to the younger Nold seniors, the older ones were characterized by a lower global magnitude of the rsEEG alpha rhythms at the scalp sensors. Notably, this effect was mainly evident in posterior (eLORETA) cortical sources estimated from those alpha rhythms.

The present results confirm previous findings showing that the physiological aging is related to less evident alpha waveforms and power density in rsEEG rhythms recorded in Nold seniors [4, 11, 13, 14, 19, 65], especially at the scalp electrodes placed in posterior regions [15]. The present results also extend previous findings by our research group showing a decline in posterior cortical sources of rsEEG alpha rhythms estimated in Nold seniors compared to healthy young adults [17].

Keeping in mind the above results, we posit that both global rsEEG alpha power density and its posterior cortical sources might be useful in clinical research to monitor aging effects on cortical neural synchronization mechanisms regulating brain arousal and vigilance in quiet wakefulness as basis for Nold seniors' global cognitive status [39]. They may be combined with rsEEG biomarkers in other frequency bands typically deranging with age in Nold seniors [66–69]. In this vein, previous rsEEG studies in Nold seniors reported that intermittent temporal delta or theta rhythms may be associated with WM hyperintensities or neurodegenerative processes as revealed by structural MRIs [7, 68, 70], especially when several features indicating their benign nature are not observed [7]. Another rsEEG study considering delta to beta rhythms in Nold seniors reported that an increase in posterior delta rhythms was associated to cognitive decline and reduced acetylcholinesterase activity in the CSF [19]. Furthermore, an rsEEG study in Nold seniors > 90 years reported abnormalities in delta and/or alpha rhythms in the majority of them [67]. Moreover, an MRI study in Nold seniors showed that the DMN and MM microstructure progressively deranged with the age [36]. In the same line, the atrophy of medial-temporal, parietal, and cingulate cortical areas also showed a progressive increase in Nold seniors at the follow-up [34].

Keeping in mind the above data and considerations, future rsEEG studies in Nold seniors may take into account the following variables to improve the monitoring of pathological brain aging: 1) delta-theta and posterior alpha power density measures computed on individual basis based on the TF and IAFp [4]; 2) broad range of ages > 50 years including Nold persons over 90s; 3) AD-related biomarkers based on

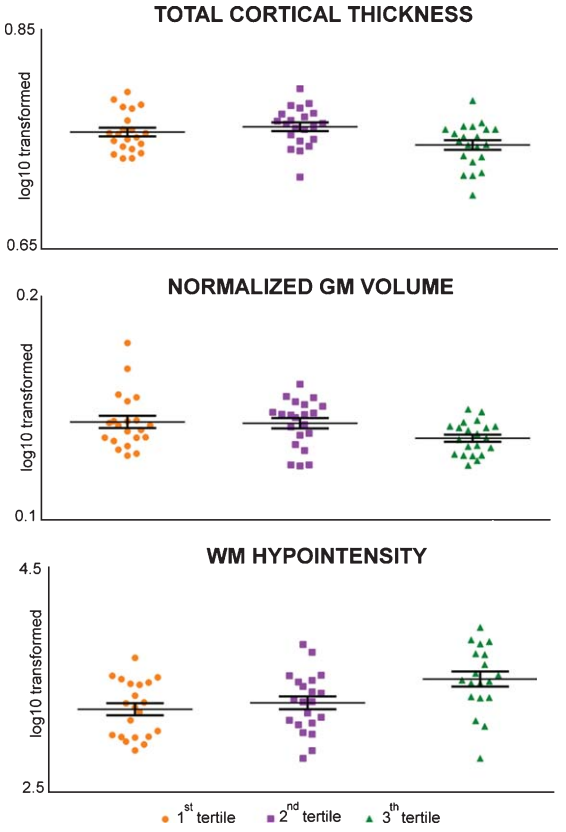

Fig. 9. Individual values (log-10 transformed) of the total grey matter (GM) volume, total cortical thickness, and white matter (WM) hypointensity in the three subgroups of the ADMCI patients (1st, 2nd, and 3rd tertiles).

CSF and MRI measures (e.g., Aβ_{42}, p-tau, t-tau, cortical GM thickness and volumes, acetylcholinesterase activity, WM hyperintensity, etc.) for stratifying Nold seniors in those being positive versus negative to those biomarkers; and 4) well-known risk factors of neurodegenerative dementing disorders such as blood hypertension, diabetes, obesity, chronic neuroinflammation, chronic kidney diseases, subtle depression, and sleep disorders for stratification of Nold seniors in those being positive versus negative to those risk factors [71, 72]. Future studies should also consider that even "statistically normal" rsEEG rhythms might not exclude the existence of brain neuropathological processes.

AD variants overwhelm aging effects on rsEEG alpha rhythms in ADMCI patients

In the present ADMCI patients, the age factor did affect neither the TF nor the IAFp. In contrast, it affected the magnitude of rsEEG alpha rhythms interacting with the disease. As compared to the younger ADMCI patients, the older ones (matched as education, gender, and global cognitive status) were characterized by a paradoxical smaller abnormality in the global magnitude of rsEEG alpha rhythms at the scalp sensors. This effect was mainly evident in the alpha posterior cortical sources, partially in agreement with previous evidence showing that abnormalities in rsEEG delta and alpha rhythms were more pronounced in younger than older ADD patients [73]. Therefore, the rsEEG alpha rhythms may be more affected by the early-onset than the late-onset ADMCI.

Notably, the paradoxical aging effects on rsEEG activity observed in the present ADMCI patients did not depend on group differences in the following AD hallmarks: (1) *APOE4* genetic risk of sporadic AD; (2) CSF (i.e., A β_{42}, p-tau, t-tau) markers of AD neuropathology; and 3) MRI markers of structural brain impairment such as brain GM and WM volumes, the ventricular brain volume, and brain WM hyperintensities. Consistently, here we report no aging effects on the rsEEG delta-theta source activities, typically related to the mentioned AD hallmarks in ADMCI and ADD patients [25, 31, 33, 74, 75].

The lack of aging effects on the MRI biomarkers measured in the present ADMCI groups apparently contrasts with previous findings. In an MRI study in ADMCI seniors, the medial temporal, parietal, and cingulate cortical areas showed increased atrophy related to age [34]. In another MRI study, the hippocampus and amygdala exhibited more atrophy over time in younger (but not older) ADMCI patients with *APOE4* than without *APOE4* [38]. Furthermore, even stronger age effects were found in ADD patients. In an MRI study in ADD patients, addictive aging and AD factors significantly affected GM atrophy in many brain regions [35]. In another MRI study, there was a marked association between the GM atrophy in brain regions and cognitive deficits in several domains in younger ADD patients suffering from an early-onset disease [76]. In the same study, the late onset ADD patients also manifested an association between global cerebral atrophy and episodic memory impairment [76]. Finally, further MRI evidence showed that early-onset and late-onset ADD patients were characterized by different cortical and subcortical atrophy [77, 78].

Why did not we see relationships among age, MRI, and *APOE4* biomarkers in the present ADMCI patients? It can be speculated that this lack of relationships may be due to their relatively high

Table 9
Results of the linear regression models evaluating the association between the age and the global rsEEG alpha 2 and 3 scalp normalized power density in the Nold and ADMCI groups

Dependent Variable	Predictors	Beta coefficient	t-statistics (p)	Lower Confidence Interval (95%)	Upper Confidence Interval (95%)
			Nold		
Global alpha 2	*Intercept*	0.681	t = 19.032, $p = 0.0001$	0.609	0.752
	Age group = First tertile	0.155	t = 3.060, $p = 0.003$	0.053	0.256
	Age group = Second tertile	0.093	n.s.	–0.009	0.194
Global alpha 2	*Intercept*	1.414	t = 6.414, $p = 0.0001$	0.972	1.856
	Age	–0.009	t = –2.960, $p = 0.004$	–0.016	–0.003
Global alpha 3	*Intercept*	0.609	t = 17.499, $p = 0.0001$	0.539	0.678
	Age group = First tertile	0.146	t = 2.979, $p = 0.004$	0.048	0.245
	Age group = Second tertile	0.120	t = 2.443, $p = 0.018$	0.022	0.219
Global alpha 3	*Intercept*	1.391	t = 6.539, $p = 0.0001$	0.965	1.816
	Age	–0.010	t = –3.274, $p = 0.002$	–0.016	–0.004
			ADMCI		
Global alpha 2	*Intercept*	0.734	t = 15.635, $p = 0.0001$	0.640	0.828
	Age group = First tertile	–0.239	t = –3.604, $p = 0.001$	–0.372	–0.106
	Age group = Second tertile	–0.190	t = –2.860, $p = 0.006$	–0.323	–0.057
Global alpha 2	*Intercept*	–0.307	n.s.	–0.932	0.318
	Age	0.013	t = 2.885, $p = 005$	0.004	0.022
Global alpha 3	*Intercept*	0.632	t = 13.797, $p = 0.0001$	0.541	0.724
	Age group = First tertile	–0.183	t = –2.819, $p = 0.007$	–0.312	–0.053
	Age group = Second tertile	–0.121	n.s.	–0.250	0.009
Global alpha 3	*Intercept*	–0.113	n.s.	–0.714	0.487
	Age	0.009	t = 2.157, $p = 04$	0.001	0.018
Global alpha 2	*Age groups*APOE4*	000005	n.s.	–0.023	0.024
Global alpha 3	*Age groups*APOE4*	–0.0005	n.s.	–0.023	0.023

education attainment and mild clinical manifestations. Indeed, they showed a mean MMSE score > 25 corrected by the age (best cognitive status = 30) and about 11 years of mean education attainment. Such attainment may be related to a significant cognitive reserve and premorbid intelligence that may compensate for the natural derangement of brain structure and function with age [79]. In this speculative line, previous evidence showed that high education attainment might partially counteract structural brain lesions as revealed by MRI biomarkers in AD patients, thus delaying the onset of MCI and dementia in seniors with remarkable cerebral abnormalities [80, 81]. Furthermore, compared to ADMCI patients with low education attainment, those with high education attainment showed similar cognitive deficits despite greater macroscopic WM lesions [82]. Future cross-sectional studies may test this speculative explanation. To this aim, the effects of age and education attainment on rsEEG and neuroimaging biomarkers may be investigated in AD patients enrolled at the clinical stages of pre-MCI, MCI, mild and moderate ADD as a function of both.

A tentative neurophysiological model

At the present early stage of the research, we poorly know what neurophysiological aging mechanisms may induce abnormalities in rsEEG alpha rhythms recorded in Nold and ADMCI seniors as a function of aging and disease variants. As part of the scientific challenge, those mechanisms may be sensitive to both constitutional and environmental factors and may operate in the brain at various spatial scales [83, 84].

According to the present neurophysiological approach, here we discuss age-related neurophysiological mechanisms affecting rsEEG alpha rhythms at a large spatial macroscale involving multiple subcortical and cortical oscillating circuits. Those neurophysiological mechanisms may modulate delays in the synchronization at alpha frequencies of the neural activity within ascending brain networks [85, 86]. At the cellular and molecular level, these networks may include reciprocal thalamus and cortical loops formed by thalamocortical high-threshold glutamatergic neurons, thalamocortical relay-mode glutamatergic neurons, reticular thalamic

GABAergic neurons, and corticothalamic pyramidal glutamatergic neurons [85, 87, 88]. Furthermore, they may include ascending activating reticular systems mainly shaped by brainstem noradrenergic and dopaminergic neurons as well as basal forebrain cholinergic neurons [85, 87].

In physiological conditions, these brain networks might enhance the (inhibitory) synchronization at alpha frequencies of cortical neurons not actually involved in the active information processing, thus reducing cortical neural noise and making more efficient the activation of relevant cortical neural populations in response to actual sensory and cognitive-motor events [85, 87, 89]. During physiological aging, the efficiency of that synchronization may be reduced in Nold (and ADMCI) seniors. It may partially derange alpha rhythms in target occipital-parietal visual and visuospatial cortical areas, possibly interfering with the event-related desynchronization of alpha rhythms underpinning attention and sensory-motor information processing [1, 8, 89, 90].

In this physiological aging mechanism, it can be speculated that a prominent role may be played by the progressive loss of cholinergic basal forebrain projections to the thalamus and posterior cerebral cortex. In a recent study, both young adults and Nold seniors showed that functional rsMRI connectivity between the cholinergic basal forebrain and the occipital cortex increased from the eyes-closed to the eyes-open condition proportionally to the reduction in amplitude of rsEEG alpha rhythms [86]. In the Nold seniors, lesions in the WM connectivity between the cholinergic basal forebrain and the occipital cortex were related to a reduction of rsEEG alpha reactivity to eye opening [86].

In the case of early-onset AD, the above subcortical-cortical neural systems generating rsEEG alpha rhythms might be especially impaired. In a previous neuroimaging (MRI-PET) study, abnormalities in subcortical structures (amygdala, caudate, and putamen) were more widely associated with AD hallmarks (amyloidosis, tauopathy, and atrophy) and multi-domain cognitive impairment in early-onset than late-onset ADD patients [91]. As compared to the late-onset ADD patients, the early-onset ADD patients also showed a more rapid cognitive impairment (attention, language, and frontal-executive) related to the volumetric decline in subcortical (caudate, putamen, and thalamus) and cortical associative regions at 3-year follow-up [92, 93]. Following this "subcortical" hypothesis, it can be speculated that as compared to the late-onset ADMCI patients, the early-onset ADMCI patients may suffer from prominent abnormalities in the rsEEG alpha rhythms related to greater alterations in the cholinergic ascending systems to the cerebral cortex. In this vein, a previous study showed greater alterations in those systems and posterior rsEEG alpha rhythms in ADMCI and ADD patients [94]. Furthermore, the chronic administration of Donepezil (an acetylcholinesterase inhibitor licensed for the treatment of ADMCI and ADD patients) showed specific beneficial effects on posterior rsEEG alpha rhythms and global cognitive status in ADMCI and ADD patients [95].

Methodological remarks

The clinical 10–20 electrode montage (i.e., 19 scalp electrodes) adopted for the present rsEEG recordings is suboptimal for accurate rsEEG source estimations [96, 97], as an optimal rsEEG spatial sampling would require >64 scalp electrodes [96, 97]. Therefore, the present spatial analysis of age-related effects on rsEEG cortical sources should be considered explorative.

Important critical aspects of the present individual spectral analysis are the following: 1) We divided the alpha band into sub-bands because of, in the eyes-closed rsEEG condition, dominant low-frequency alpha rhythms (alpha 1 and alpha 2) may denote the synchronization of diffuse neural networks regulating the fluctuation of the subject's global awake and conscious states, while high-frequency alpha rhythms (alpha 3) may denote the synchronization of more selective neural networks specialized in the processing of modal specific or semantic information [4, 89]. When the subject is engaged in sensorimotor or cognitive tasks, alpha and low-frequency beta (beta 1) rhythms reduce in power (i.e., desynchronization or blocking) and are replaced by fast EEG oscillations at high-frequency beta (beta 2) and gamma rhythms [89]. 2) We considered individual delta, theta, and alpha frequency bands because a clinical group may be characterized by a mean slowing in the peak frequency of the alpha power density without any substantial change in the magnitude of the power density. In that specific case, the use of fixed frequency bands would result in a statistical effect erroneously showing alpha power density values lower in the clinical than the control group; 3) We used fixed frequency ranges for the beta and gamma bands because the individual beta and gamma frequency peaks were

evident only in a few subjects (< 10%); and 4) We selected the beginning of the beta frequency range at 14 Hz to avoid the overlapping between individual alpha and fixed beta frequency ranges (i.e., individual alpha frequency band ranged from TF to 14 Hz with an IAFp = 12 Hz). The interpretation of the present results should consider the above methodological options.

Another significant methodological limitation is the availability of the rsEEG recordings only at a single data acquisition session, thus preventing the evaluation of the relationship between the age and the deterioration over time in the rsEEG alpha rhythms recorded in Nold and ADMCI seniors.

The above methodological limitations motivate resource investments to develop future prospective, longitudinal, and multi-center studies using 1) harmonized EEG hardware systems and clinical protocols; () a higher number of exploring scalp electrodes for spatially enhanced rsEEG source estimates; and 3) at least 2 follow-ups better capturing the effects of the age on rsEEG alpha rhythms in both Nold and ADMCI seniors.

CONCLUSIONS

Here, we tested whether the age may differently affect rsEEG alpha rhythms in Nold and ADMCI persons.

As compared to the younger Nold seniors, the older ones showed greater reductions in rsEEG alpha rhythms with major topographical effects in posterior regions. On the contrary, in relation to the younger ADMCI patients, the older ones displayed lesser reductions in those rhythms. Notably, these results in the ADMCI patients were not affected by CSF AD-related diagnostic biomarkers, GM and WM brain lesions, and clinical and neuropsychological scores.

The results of the present study suggest that in Nold seniors, the aging factor may significantly affect neurophysiological brain neural synchronization mechanisms underpinning the generation of dominant rsEEG alpha rhythms for the regulation of cortical arousal during the quiet vigilance. In contrast, rsEEG alpha rhythms recorded in ADMCI patients may be more affected by the disease variants, with more deleterious effects observed in early- than the late-onset ADMCI patients. In the ADMCI patients, the mere effects of the aging factor may be hidden by dysfunctions in subcortical structures, including the cholinergic basal forebrain and thalamus.

Keeping in mind the above data and considerations, the present rsEEG measures may be included in an ideal biomarker panel for future longitudinal clinical trials involving both Nold and ADMCI groups of seniors. These measures may account for the aging and disease effects on the neurophysiological mechanisms underpinning brain arousal and vigilance, in line with the recent recommendations by an Expert Workgroup of the Electrophysiology Professional Interest of Alzheimer's Association [39].

ACKNOWLEDGMENTS

The present study was developed based on the database of The PDWAVES Consortium (http://www.pdwaves.eu) with some datasets of the FP7-IMI "PharmaCog" (http://www.pharmacog.org) project. The members and institutional affiliations of the Clinical Units are reported on the cover page of this manuscript. In this study, the electroencephalographic data analysis was partially supported by the funds of "Ricerca Corrente" attributed by the Italian Ministry of Health to the IRCCS SDN of Naples, IRCCS OASI Maria SS of Troina, and IRCCS San Raffaele Pisana of Rome.

Authors' disclosures available online (https://www.j-alz.com/manuscript-disclosures/20-1271r1).

REFERENCES

[1] Babiloni C, Barry RJ, Başar E, Blinowska KJ, Cichocki A, Drinkenburg WHIM, Klimesch W, Knight RT, Lopes da Silva F, Nunez P, Oostenveld R, Jeong J, Pascual-Marqui R, Valdes-Sosa P, Hallett M (2020) International Federation of Clinical Neurophysiology (IFCN) - EEG research workgroup: Recommendations on frequency and topographic analysis of resting state EEG rhythms. Part 1: Applications in clinical research studies. *Clin Neurophysiol* **131**, 285-307.

[2] Del Percio C, Infarinato F, Iacoboni M, Marzano N, Soricelli A, Aschieri P, Eusebi F, Babiloni C (2010) Movement-related desynchronization of alpha rhythms is lower in athletes than non-athletes: A high-resolution EEG study. *Clin Neurophysiol* **121**, 482-491.

[3] Klimesch W (2012) α-band oscillations, attention, and controlled access to stored information. *Trends Cogn Sci* **16**, 606-617.

[4] Klimesch W (1999) EEG alpha and theta oscillations reflect cognitive and memory performance: A review and analysis. *Brain Res Rev* **29**, 169-195.

[5] Srinivasan R, Bibi FA, Nunez PL (2006) Steady-state visual evoked potentials: Distributed local sources and wave-like dynamics are sensitive to flicker frequency. *Brain Topogr* **18**, 167-187.

[6] Steriade M (2003) The corticothalamic system in sleep. *Front Biosci* **8**, 878-899.

[7] Klass DW, Brenner RP (1995) Electroencephalography of the elderly. *J Clin Neurophysiol* **12**, 116-131.

[8] Babiloni C, Blinowska K, Bonanni L, Cichocki A, De Haan W, Del Percio C, Dubois B, Escudero J, Fernández A, Frisoni G, Guntekin B, Hajos M, Hampel H, Ifeachor E, Kilborn K, Kumar S, Johnsen K, Johannsson M, Jeong J, LeBeau F, Lizio R, Lopes da Silva F, Maestú F, McGeown WJ, McKeith I, Moretti DV, Nobili F, Olichney J, Onofrj M, Palop JJ, Rowan M, Stocchi F, Struzik ZM, Tanila H, Teipel S, Taylor JP, Weiergräber M, Yener G, Young-Pearse T, Drinkenburg WH, Randall F (2020) What electrophysiology tells us about Alzheimer's disease: A window into the synchronization and connectivity of brain neurons. *Neurobiol Aging* **85**, 58-73.

[9] Rossini PM, Di Iorio R, Vecchio F, Anfossi M, Babiloni C, Bozzali M, Bruni AC, Cappa SF, Escudero J, Fraga FJ, Giannakopoulos P, Guntekin B, Logroscino G, Marra C, Miraglia F, Panza F, Tecchio F, Pascual-Leone A, Dubois B (2020) Early diagnosis of Alzheimer's disease: The role of biomarkers including advanced EEG signal analysis. Report from the IFCN-sponsored panel of experts. *Clin Neurophysiol* **131**, 1287-1310.

[10] Hubbard O, Sunde D, Goldensohn ES (1976) The EEG in centenarians. *Electroencephalogr Clin Neurophysiol* **40**, 407-417.

[11] Knyazeva MG, Barzegaran E, Vildavski VY, Demonet JF (2018) Aging of human alpha rhythm. *Neurobiol Aging* **69**, 261-273.

[12] Markand ON (1990) Alpha rhythms. *J Clin Neurophysiol* **7**, 163-190.

[13] Müller V, Lindenberger U (2012) Lifespan differences in nonlinear dynamics during rest and auditory oddball performance. *Dev Sci* **15**, 540-556.

[14] Gaál ZA, Boha R, Stam CJ, Molnár M (2010) Age-dependent features of EEG-reactivity—Spectral, complexity, and network characteristics. *Neurosci Lett* **479**, 79-84.

[15] Dustman RE, LaMarche JA, Cohn NB, Shearer DE, Talone JM (1985) Power spectral analysis and cortical coupling of EEG for young and old normal adults. *Neurobiol Aging* **6**, 193-198.

[16] Aird RB, Gastaut Y (1959) Occipital and posterior electroencephalographic rhythms. *Electroencephalogr Clin Neurophysiol* **11**, 637-656.

[17] Babiloni C, Binetti G, Cassarino A, Dal Forno G, Del Percio C, Ferreri F, Ferri R, Frisoni G, Galderisi S, Hirata K, Lanuzza B, Miniussi C, Mucci A, Nobili F, Rodriguez G, Luca Romani G, Rossini PM (2006) Sources of cortical rhythms in adults during physiological aging: A multicentric EEG study. *Hum Brain Mapp* **27**, 162-172.

[18] Caplan JB, Bottomley M, Kang P, Dixon RA (2015) Distinguishing rhythmic from non-rhythmic brain activity during rest in healthy neurocognitive aging. *Neuroimage* **112**, 341-352.

[19] Hartikainen P, Soininen H, Partanen J, Helkala E, Riekkinen P (1992) Aging and spectral analysis of EEG in normal subjects: A link to memory and CSF AChE. *Acta Neurol Scand* **86**, 148-155.

[20] Adler G, Brassen S, Jajcevic A (2003) EEG coherence in Alzheimer's dementia. *J Neural Transm* **110**, 1051-1058.

[21] Zan der Hiele K, Vein AA, Reijntjes RH, Westendorp RG, Bollen EL, van Buchem MA, van Dijk JG, Middelkoop HA (2007) EEG correlates in the spectrum of cognitive decline. *Clin Neurophysiol* **118**, 1931-1939.

[22] Babiloni C, Binetti G, Cassetta E, Cerboneschi D, Dal Forno G, Del Percio C, Ferreri F, Ferri R, Lanuzza B, Miniussi C, Moretti DV, Nobili F, Pascual-Marqui RD, Rodriguez G, Romani GL, Salinari S, Tecchio F, Vitali P, Zanetti O, Zappasodi F, Rossini PM (2004) Mapping distributed sources of cortical rhythms in mild Alzheimer's disease. A multicentric EEG study. *Neuroimage* **22**, 57-67.

[23] Babiloni C, Lizio R, Vecchio F, Frisoni GB, Pievani M, Geroldi C, Claudia F, Ferri R, Lanuzza B, Rossini PM (2010) Reactivity of cortical alpha rhythms to eye opening in mild cognitive impairment and Alzheimer's disease: An EEG study. *J Alzheimers Dis* **22**, 1047-1064.

[24] Babiloni C, Vecchio F, Lizio R, Ferri R, Rodriguez G, Marzano N, Frisoni GB, Rossini PM (2011) Resting state cortical rhythms in mild cognitive impairment and Alzheimer's disease: Electroencephalographic evidence. *J Alzheimers Dis* **3**, 201-214.

[25] Babiloni C, Carducci F, Lizio R, Vecchio F, Baglieri A, Bernardini S, Cavedo E, Bozzao A, Buttinelli C, Esposito F, Giubilei F, Guizzaro A, Marino S, Montella P, Quattrocchi CC, Redolfi A, Soricelli A, Tedeschi G, Ferri R, Rossi-Fedele G, Ursini F, Scrascia F, Vernieri F, Pedersen TJ, Hardemark HG, Rossini PM, Frisoni GB (2013) Resting state cortical electroencephalographic rhythms are related to gray matter volume in subjects with mild cognitive impairment and Alzheimer's disease. *Hum Brain Mapp* **34**, 1427-1446.

[26] Babiloni C, Del Percio C, Bordet R, Bourriez JL, Bentivoglio M, Payoux P, Derambure P, Dix S, Infarinato F, Lizio R, Triggiani AI, Richardson JC, Rossini PM (2013) Effects of acetylcholinesterase inhibitors and memantine on resting-state electroencephalographic rhythms in Alzheimer's disease patients. *Clin Neurophysiol* **124**, 837-850.

[27] Canuet L, Tellado I, Couceiro V, Fraile C, Fernandez-Novoa L, Ishii R, Takeda M, Cacabelos R (2012) Resting-state network disruption and APOE genotype in Alzheimer's disease: A lagged functional connectivity study. *PLoS One* **7**, 46289.

[28] Dierks T, Ihl R, Frölich L, Maurer K (1993) Dementia of the Alzheimer type: Effects on the spontaneous EEG described by dipole sources. *Psychiatry Res* **50**, 151-162.

[29] Huang C, Wahlund L, Dierks T, Julin P, Winblad B, Jelic V (2000) Discrimination of Alzheimer's disease and mild cognitive impairment by equivalent EEG sources: A cross-sectional and longitudinal study. *Clin Neurophysiol* **111**, 1961-1967.

[30] Babiloni C, Visser PJ, Frisoni G, De Deyn PP, Bresciani L, Jelic V, Nagels G, Rodriguez G, Rossini PM, Vecchio F, Colombo D, Verhey F, Wahlund LO, Nobili F (2010) Cortical sources of resting EEG rhythms in mild cognitive impairment and subjective memory complaint. *Neurobiol Aging* **31**, 1787-1798.

[31] Babiloni C, Benussi L, Binetti G, Bosco P, Busonero G, Cesaretti S, Dal Forno G, Del Percio C, Ferri R, Frisoni G, Ghidoni R, Rodriguez G, Squitti R, Rossini PM (2006) Genotype (cystatin C) and EEG phenotype in Alzheimer disease and mild cognitive impairment: A multicentric study. *Neuroimage* **29**, 948-964.

[32] Babiloni C, Benussi L, Binetti G, Cassetta E, Dal Forno G, Del Percio C, Ferreri F, Ferri R, Frisoni G, Ghidoni R, Miniussi C, Rodriguez G, Romani GL, Squitti R, Ventriglia MC, Rossini PM (2006) Apolipoprotein E and alpha brain rhythms in mild cognitive impairment: A multicentric electroencephalogram study. *Ann Neurol* **59**, 323-334.

[33] Jovicich J, Babiloni C, Ferrari C, Marizzoni M, Moretti DV, Del Percio C, Lizio R, Lopez S, Galluzzi S, Albani D, Cavaliere L, Minati L, Didic M, Fiedler U, Forloni G, Hensch T, Molinuevo JL, Bartrés Faz D, Nobili F,

Orlandi D, Parnetti L, Farotti L, Costa C, Payoux P, Rossini PM, Marra C, Schönknecht P, Soricelli A, Noce G, Salvatore M, Tsolaki M, Visser PJ, Richardson JC, Wiltfang J, Bordet R, Blin O, Frisoniand GB; and the PharmaCog Consortium (2019) Two-year longitudinal monitoring of amnestic mild cognitive impairment patients with prodromal Alzheimer's disease using topographical biomarkers derived from functional magnetic resonance imaging and electroencephalographic activity. *J Alzheimers Dis* **69**, 15-35.

[34] Rhodius-Meester HFM, Benedictus MR, Wattjes MP, Barkhof F, Scheltens P, Muller M, van der Flier WM (2017) MRI visual ratings of brain atrophy and white matter hyperintensities across the spectrum of cognitive decline are differently affected by age and diagnosis. *Front Aging Neurosci* **9**, 117.

[35] Pichet Binette A, Gonneaud J, Vogel JW, La Joie R, Rosa-Neto P, Collins DL, Poirier J, Breitner JCS, Villeneuve S, Vachon-Presseau E; Alzheimer's Disease Neuroimaging Initiative; PREVENT-AD Research Group (2020) Morphometric network differences in ageing versus Alzheimer's disease dementia. *Brain* **143**, 635-649.

[36] Brown CA, Jiang Y, Smith CD, Gold BT (2018) Age and Alzheimer's pathology disrupt default mode network functioning via alterations in white matter microstructure but not hyperintensities. *Cortex* **104**, 58-74.

[37] Harrison TM, La Joie R, Maass A, Baker SL, Swinnerton K, Fenton L, Mellinger TJ, Edwards L, Pham J, Miller BL, Rabinovici GD, Jagust WJ (2019) Longitudinal tau accumulation and atrophy in aging and Alzheimer disease. *Ann Neurol* **85**, 229-240.

[38] Tang X, Holland D, Dale AM, Miller MI; Alzheimer's Disease Neuroimaging Initiative (2015) APOE affects the volume and shape of the amygdala and the hippocampus in mild cognitive impairment and Alzheimer's disease: Age matters. *J Alzheimers Dis* **47**, 645-660.

[39] Babiloni C, Arakaki X, Azami H, Bennys K, Blinowska K, Bonanni L, Bujan A, Carrillo MC, Cichocki A, de Frutos-Lucas J, Del Percio C, Dubois B, Edelmayer R, Egan G, Epelbaum S, Escudero J, Evans A, Farina F, Fargo K, Fernández A, Ferri R, Frisoni G, Hampel H, Harrington MG, Jelic V, Jeong J, Jiang Y, Kaminski M, Kavcic V, Kilborn K, Kumar S, Lam A, Lim L, Lizio R, Lopez D, Lopez S, Lucey B, Maestú F, McGeown WJ, McKeith I, Moretti DV, Nobili F, Noce G, Olichney J, Onofrj M, Osorio R, Parra-Rodriguez M, Rajji T, Ritter P, Soricelli A, Stocchi F, Tarnanas I, Taylor JP, Teipel S, Tucci F, Valdes-Sosa M, Valdes-Sosa P, Weiergräber M, Yener G, Guntekin B (2021) Measures of resting state EEG rhythms for clinical trials in Alzheimer's disease: Recommendations of an expert panel. *Alzheimers Dement*, doi: 10.1002/alz.12311

[40] Albert MS, DeKosky ST, Dickson D, Dubois B, Feldman HH, Fox NC, Gamst A, Holtzman DM, Jagust WJ, Petersen RC, Snyder PJ, Carrillo MC, Thies B, Phelps CH (2011) The diagnosis of mild cognitive impairment due to Alzheimer's disease: Recommendations from the National Institute on Aging-Alzheimer's Association workgroups on diagnostic guidelines for Alzheimer's disease. *Alzheimers Dement* **7**, 270-279.

[41] Morris JC (1993) The Clinical Dementia Rating (CDR): Current version and scoring rules. *Neurology* **43**, 2412-2414.

[42] Wechsler D (1987) *Manual for the Wechsler Memory Scale-Revised*. The Psychological Corporation, San Antonio, TX.

[43] Brown LM, Schinka JA (2005) Development and initial validation of a 15-item informant version of the geriatric depression scale. *Int J Getriatr Psychiatry* **20**, 911-918.

[44] Rosen WG, Terry RD, Fuld PA, Katzman R, Peck A (1980) Pathological verification of ischemic score in differentiation of dementias. *Ann Neurol* **7**, 486-488.

[45] Jack, CR, Bennett DA, Blennow K, Carrillo MC, Dunn B, Haeberlein SB, Holtzman DM, Jagust W, Jessen F, Karlawish J, Liu E, Molinuevo JL, Montine T, Phelps C, Rankin KP, Rowe CC, Scheltens P, Siemers E, Snyder HM, Sperling R (2018). NIA-AA Research Framework: Toward a biological definition of Alzheimer's disease. *Alzheimers Dement* **14**, 535-562.

[46] Mattsson N (2011) CSF biomarkers in neurodegenerative diseases. *Clin Chem Lab Med* **49**, 345-352.

[47] Marizzoni M, Ferrari C, Babiloni C, Albani D, Barkhof F, Cavaliere L, Didic M, Forloni G, Fusco F, Galluzzi S, Hensch T, Jovicich J, Marra C, Molinuevo JL, Nobili F, Parnetti L, Payoux P, Ranjeva JP, Ribaldi F, Rolandi E, Rossini PM, Salvatore M, Soricelli A, Tsolaki M, Visser PJ, Wiltfang J, Richardson JC, Bordet R, Blin O, Frisoni GB (2020) CSF cutoffs for MCI due to AD depend on APOEε4 carrier status. *Neurobiol Aging* **89**, 55-62.

[48] Fischl B, Salat DH, van der Kouwe AJ, Makris, N, Segonne F, Quinn BT, Dale AM (2004) Sequence-independent segmentation of magnetic resonance images. *NeuroImage* **23**, S69–S84.

[49] Desikan RS, Ségonne F, Fischl B, Quinn BT, Dickerson BC, Blacker D, Buckner RL, Dale AM, Maguire RP, Hyman BT, Albert MS, Killiany RJ (2006) An automated labeling system for subdividing the human cerebral cortex on MRI scans into gyral based regions of interest. *Neuroimage* **31**, 968–980.

[50] Rosen WG, Mohs RC, Davis KL (1984) A new rating scale for Alzheimer's disease. *Am J Psychiatry* **141**, 1356-1364.

[51] Folstein MF, Folstein SE, McHugh PR (1975) "Mini-mental state". A practical method for grading the cognitive state of patients for the clinician. *J Psychiatr Res* **12**, 189-198.

[52] Rey A (1968) *Reattivo della figura complessa*. Organizzazioni Speciali, Firenze.

[53] Reitan RM (1958) Validity of the Trail Making Test as an indicator of organic brain damage. *Percept Mot Skills* **8**, 271-276.

[54] Novelli G, Papagno C, Capitani E, Laiacona M, Vallar G, Cappa SF (1986) Tre test clinici di ricerca e produzione lessicale. Taratura su soggetti normali. *Arch Psicol Neurol Psichiatr* **47**, 477-506.

[55] Freedman M, Leach L, Kaplan E, Winoucur G, Shulman KJ, Delis DC (1994) *Clock Drawing. A neuropsychological analysis*. Oxford University Press, New York.

[56] Babiloni C, Del Percio C, Lizio R, Noce G, Lopez S, Soricelli A, Ferri R, Pascarelli MT, Catania V, Nobili F, Arnaldi D, Famà F, Aarsland D, Orzi F, Buttinelli C, Giubilei F, Onofrj M, Stocchi F, Vacca L, Stirpe P, Fuhr P, Gschwandtner U, Ransmayr G, Garn H, Fraioli L, Pievani M, Frisoni GB, D'Antonio F, De Lena C, Güntekin B, Hanoğlu L, Başar E, Yener G, Emek-Savaş DD, Triggiani AI, Franciotti R, Taylor JP, De Pandis MF, Bonanni L (2017) Abnormalities of cortical neural synchronization mechanisms in subjects with mild cognitive impairment due to Alzheimer's and Parkinson's diseases: An EEG study. *J Alzheimers Dis* **59**, 339-358.

[57] Babiloni C, Del Percio C, Lizio R, Noce G, Lopez S, Soricelli A, Ferri R, Pascarelli MT, Catania V, Nobili F, Arnaldi D, Famà F, Aarsland D, Orzi F, Buttinelli C, Giubilei F,

Onofrj M, Stocchi F, Vacca L, Stirpe P, Fuhr P, Gschwandtner U, Ransmayr G, Garn H, Fraioli L, Pievani M, Frisoni GB, D'Antonio F, De Lena C, Güntekin B, Hanoğlu L, Başar E, Yener G, Emek-Savaş DD, Triggiani AI, Franciotti R, Taylor JP, De Pandis MF, Bonanni L (2018) Abnormalities of resting state cortical EEG rhythms in subjects with mild cognitive impairment due to Alzheimer's and Lewy body diseases. *J Alzheimers Dis* **62**, 247-268.

[58] Salinsky MC, Oken BS, Morehead L (1991) Test-retest reliability in EEG frequency analysis. *Electroencephalogr Clin Neurophysiol* **79**, 382-392.

[59] Babiloni C, Del Percio C, Lizio R, Noce G, Lopez S, Soricelli A, Ferri R, Pascarelli MT, Catania V, Nobili F, Arnaldi D, Famà F, Orzi F, Buttinelli C, Giubilei F, Bonanni L, Franciotti R, Onofrj M, Stirpe P, Fuhr P, Gschwandtner U, Ransmayr G, Garn H, Fraioli L, Pievani M, D'Antonio F, De Lena C, Güntekin B, Hanoğlu L, Başar E, Yener G, Emek-Savaş DD, Triggiani AI, Taylor JP, De Pandis MF, Vacca L, Frisoni GB, Stocchi F (2018) Functional cortical source connectivity of resting state electroencephalographic alpha rhythms shows similar abnormalities in patients with mild cognitive impairment due to Alzheimer's and Parkinson's diseases. *Clin Neurophysiol* **129**, 766-782.

[60] Klimesch W, Doppelmayr M, Russegger H, Pachinger T, Schwaiger J (1998) Induced alpha band power changes in the human EEG and attention. *Neurosci Lett* **244**, 73-76.

[61] Klimesch W, Doppelmayr M, Russegger H, Pachinger T (1996) Theta band power in the human scalp EEG and the encoding of new information. *Neuroreport* **7**, 1235-1240.

[62] Pascual-Marqui RD (2007) Discrete, 3D distributed, linear imaging methods of electric neuronal activity. Part 1: Exact, zero error localization. *Math Phys*, arXiv:0710.3341 [math-ph].

[63] Caltagirone C, Gainotti G, Carlesimo GA, Parnetti L, e il gruppo per la standardizzazione della batteria per il deterioramento mentale (1995) Batteria per la valutazione del deterioramento mentale (Parte I): Descrizione di uno strumento di diagnosi neuropsicologica. *Arch Psicol Neurol Psichiatr* **56**, 461-470.

[64] Watson YI, Arfken CL, Birge SJ (1993) Clock completion: An objective screening test for dementia. *J Am Geriatr Soc* **41**, 1235-1240.

[65] Markand ON (1990) Alpha rhythms. *J Clin Neurophysiol* **7**, 163-190.

[66] Obrist WD (1954) The electroencephalogram of normal aged adults. *Electroencephalogr Clin Neurophysiol* **6**, 235-244.

[67] Peltz CB, Kim HL, Kawas CH (2010) Abnormal EEGs in cognitively and physically healthy oldest old: Findings from the 90+study. *J Clin Neurophysiol* **27**, 292-295.

[68] Oken BS, Kaye JA (1992) Electrophysiologic function in the healthy, extremely old. *Neurology* **42**, 519-526.

[69] Visser S, Hooijer C, Jonker C, Van Tilburg W, De Rijke W (1987) Anterior temporal focal abnormalities in EEG in normal aged subjects; correlations with psychopathological and CT brain scan findings. *Electroencephalogr Clin Neurophysiol* **66**, 1-7.

[70] Liedorp M, van der Flier WM, Hoogervorst EL, Scheltens P, Stam CJ (2009) Associations between patterns of EEG abnormalities and diagnosis in a large memory clinic cohort. *Dement Geriatr Cogn Disord* **27**, 18-23.

[71] Daulatzai MA (2017) Cerebral hypoperfusion and glucose hypometabolism: Key pathophysiological modulators promote neurodegeneration, cognitive impairment, and Alzheimer's disease. *J Neurosci Res* **95**, 943-972.

[72] Wang M, Norman JE, Srinivasan VJ, Rutledge JC (2016) Metabolic, inflammatory, and microvascular determinants of white matter disease and cognitive decline. *Am J Neurodegener Dis* **5**, 171-177.

[73] De Waal H, Stam CJ, de Haan W, van Straaten EC, Scheltens P, van der Flier WM (2012) Young Alzheimer patients show distinct regional changes of oscillatory brain dynamics. *Neurobiol Aging* **33**, 1008.e25-31.

[74] Musaeus CS, Engedal K, Høgh P, Jelic V, Mørup M, Naik M, Oeksengaard AR, Snaedal J, Wahlund LO, Waldemar G, Andersen BB (2018) EEG theta power is an early marker of cognitive decline in dementia due to Alzheimer's disease. *J Alzheimers Dis* **64**, 1359-1371.

[75] Smailovic U, Koenig T, Kåreholt I, Andersson T, Kramberger MG, Winblad B, Jelic V (2018) Quantitative EEG power and synchronization correlate with Alzheimer's disease CSF biomarkers. *Neurobiol Aging* **63**, 88-95.

[76] Van der Vlies AE, Staekenborg SS, Admiraal-Behloul F, Prins ND, Barkhof F, Vrenken H, Reiber JH, Scheltens P, van der Flier WM (2013) Associations between magnetic resonance imaging measures and neuropsychological impairment in early and late onset Alzheimer's disease. *J Alzheimers Dis* **35**, 169-178.

[77] Frisoni GB, Pievani M, Testa C, Sabattoli F, Bresciani L, Bonetti M, Beltramello A, Hayashi KM, Toga AW, Thompson PM (2007) The topography of grey matter involvement in early and late onset Alzheimer's disease. *Brain* **130**, 720-730.

[78] Shiino A, Watanabe T, Kitagawa T, Kotani E, Takahashi J, Morikawa S, Akiguchi I (2008) Different atrophic patterns in early- and late-onset Alzheimer's disease and evaluation of clinical utility of a method of regional z-score analysis using voxel-based morphometry. *Dement Geriatr Cogn Disord* **26**, 175-186.

[79] Stern Y, Arenaza-Urquijo EM, Bartrés-Faz D, Belleville S, Cantilon M, Chetelat G, Ewers M, Franzmeier N, Kempermann G, Kremen WS, Okonkwo O, Scarmeas N, Soldan A, Udeh-Momoh C, Valenzuela M, Vemuri P, Vuoksimaa E; the Reserve, Resilience and Protective Factors PIA Empirical Definitions and Conceptual Frameworks Workgroup (2018) Whitepaper: Defining and investigating cognitive reserve, brain reserve, and brain maintenance. *Alzheimers Dement* **16**, 1305-1311.

[80] Mortamais M, Portet F, Brickman AM, Provenzano FA, Muraskin J, Akbaraly TN, Berr C, Touchon J, Bonafé A, le Bars E, Menjot de Champfleur N, Maller JJ, Meslin C, Sabatier R, Ritchie K, Artero S (2014) Education modulates the impact of white matter lesions on the risk of mild cognitive impairment and dementia. *Am J Geriatr Psychiatry* **22**, 1336-1345.

[81] Pettigrew C, Soldan A, Zhu Y, Wang MC, Brown T, Miller M, Albert M; BIOCARD Research Team (2017) Cognitive reserve and cortical thickness in preclinical Alzheimer's disease. *Brain Imaging Behav* **11**, 357-367.

[82] Serra L, Musicco M, Cercignani M, Torso M, Spanò B, Mastropasqua C, Giulietti G, Marra C, Bruno G, Koch G, Caltagirone C, Bozzali M (2015) Cognitive reserve and the risk for Alzheimer's disease: A longitudinal study. *Neurobiol Aging* **36**, 592-600.

[83] Marshall AC, Cooper NR (2017) The association between high levels of cumulative life stress and aberrant resting state EEG dynamics in old age. *Biol Psychol* **127**, 64-73.

[84] Meyers JL, Zhang J, Chorlian DB, Pandey AK, Kamarajan C, Wang JC, Wetherill L, Lai D, Chao M, Chan G, Kinreich S, Kapoor M, Bertelsen S, McClintick J, Bauer

L, Hesselbrock V, Kuperman S, Kramer J, Salvatore JE, Dick DM, Agrawal A, Foroud T, Edenberg HJ, Goate A, Porjesz B (2020) A genome-wide association study of interhemispheric theta EEG coherence: Implications for neural connectivity and alcohol use behavior. *Mol Psychiatry*, doi: 10.1038/s41380-020-0777-6

[85] Hughes SW, Crunelli V (2005) Thalamic mechanisms of EEG alpha rhythms and their pathological implications. *Neuroscientist* **11**, 357-372.

[86] Wan L, Huang H, Schwab N, Tanner J, Rajan A, Lam NB, Zaborszky L, Li CR, Price CC, Ding M (2019) From eyes-closed to eyes-open: Role of cholinergic projections in EC-to-EO alpha reactivity revealed by combining EEG and MRI. *Hum Brain Mapp* **40**, 566-577.

[87] Crunelli V, David F, Lőrincz ML, Hughes SW (2015) The thalamocortical network as a single slow wave-generating unit. *Curr Opin Neurobiol* **31**, 72-80.

[88] Vorobyov V, Bakharev B, Medvinskaya N, Nesterova I, Samokhin A, Deev A, Tatarnikova O, Ustyugov AA, Sengpiel F, Bobkova N (2019) Loss of midbrain dopamine neurons and altered apomorphine EEG effects in the 5xFAD mouse model of Alzheimer's disease. *J Alzheimers Dis* **70**, 241-256.

[89] Pfurtscheller G, Lopes da Silva FH (1999) Event-related EEG/MEG synchronization and desynchronization: Basic principles. *Clin Clin Neurophysiol* **110**, 1842-1857.

[90] Capotosto P, Babiloni C, Romani GL, Corbetta M (2009) Frontoparietal cortex controls spatial attention through modulation of anticipatory alpha rhythms. *J Neurosci* **29**, 5863-5872.

[91] Lee EC, Kang JM, Seo S, Seo HE, Lee SY, Park KH, Na DL, Noh Y, Seong JK (2020) Association of subcortical structural shapes with tau, amyloid, and cortical atrophy in early-onset and late-onset Alzheimer's disease. *Front Aging Neurosci* **12**, 563559.

[92] Cho H, Jeon S, Kang SJ, Lee JM, Lee JH, Kim GH, Shin JS, Kim CH, Noh Y, Im K, Kim ST, Chin J, Seo SW, Na DL (2013) Longitudinal changes of cortical thickness in early- versus late-onset Alzheimer's disease. *Neurobiol Aging* **34**, 1921.e9-1921.e15.

[93] Cho H, Seo SW, Kim JH, Kim C, Ye BS, Kim GH, Noh Y, Kim HJ, Yoon CW, Seong JK, Kim CH, Kang SJ, Chin J, Kim ST, Lee KH, Na DL (2013) Changes in subcortical structures in early- versus late-onset Alzheimer's disease. *Neurobiol Aging* **34**, 1740-1747.

[94] Babiloni C, Pievani M, Vecchio F, Geroldi C, Eusebi F, Fracassi C, Fletcher E, De Carli C, Boccardi M, Rossini PM, Frisoni GB (2009) White-matter lesions along the cholinergic tracts are related to cortical sources of EEG rhythms in amnesic mild cognitive impairment. *Hum Brain Mapp* **30**, 1431-1443.

[95] Babiloni C, Cassetta E, Dal Forno G, Del Percio C, Ferreri F, Ferri R, Lanuzza B, Miniussi C, Moretti DV, Nobili F, Pascual-Marqui RD, Rodriguez G, Luca Romani G, Salinari S, Zanetti O, Rossini PM (2006) Donepezil effects on sources of cortical rhythms in mild Alzheimer's disease: Responders vs. non-responders. *Neuroimage* **31**, 1650-1665.

[96] Liu AK, Dale AM, Belliveau JW (2002) Monte Carlo simulation studies of EEG and MEG localization accuracy. *Hum Brain Mapp* **16**, 47-62.

[97] Marino M, Liu Q, Brem S, Wenderoth N, Mantini D (2016) Automated detection and labeling of high-density EEG electrodes from structural MR images. *J Neural Eng* **13**, 056003.